UNIVERSITY OF OKLAHOMA

GRADUATE COLLEGE

EFFECT OF STEEL FIBER CONTENT ON MECHANICAL PROPERTIES OF NON-PROPRIETARY ULTRA-HIGH PERFORMANCE CONCRETE

A THESIS

SUBMITTED TO THE GRADUATE FACULTY

in partial fulfillment of the requirements for the

Degree of

MASTER OF SCIENCE

By

YANA DYACHKOVA
Norman, Oklahoma
2020

Downloaded from SHAREOK. Persistent Handle URL: https://hdl.handle.net/11244/325347

EFFECT OF STEEL FIBER CONTENT ON MECHANICAL PROPERTIES OF NON-PROPRIETARY ULTRA-HIGH PERFORMANCE CONCRETE

A THESIS APPROVED FOR THE

SCHOOL OF CIVIL ENGINEERING AND ENVIRONMENTAL SCIENCE

BY THE COMMITTEE CONSISTING OF

Dr.Royce Floyd, Chair

Dr. Jeffrey Volz

Dr. Musharraf Zaman

© Copyright by YANA DYACHKOVA 2020
All Rights Reserved.

Acknowledgements

I would like to acknowledge the members of the research team that helped throughout different parts of the project and helped make this thesis a success. I would also like to acknowledge Dr. Floyd, who guided me through this project as well as the rest of my thesis committee, Dr. Volz and Dr. Zaman for their encouragement and insightful comments. I would like to acknowledge the sponsors off this research who made this project possible, including ABC-UTC, ODOT, and CEES, as well as the material suppliers Dolese Bros. Co., Norchem, LafargeHolcim, and Bekaert who donated materials for this research. Thank you all for your support and this opportunity.

Table of Contents

List of Tables vii

List of Figures ix

Abstract xv

Chapter 1: Introduction 1

Chapter 2: Literature Review 4

2.1 Defining Ultra-High Performance Concrete 4

2.2 Steel Fibers in UHPC 5

2.3 Non-Proprietary UHPC Mixes 6

2.4 Existing Issues with Non-Proprietary UHPC 9

2.5 Summary 9

Chapter 3: Approach and Methods 11

3.1 Overview 11

3.2 Mixing Procedure 12

3.3 Specimen Curing 14

3.4 Specimen Testing 16

3.4.1 Flowability 16

3.4.2 Compressive Strength 17

3.4.3 Modulus of Elasticity 19

3.4.4 Splitting Tensile Strength 20

3.4.5 Flexural Strength/Modulus of Rupture 22

3.4.6 Freeze-Thaw 23

Chapter 4: Results and Discussion 27

4.1 University of Oklahoma J3 Mix 27
4.1.1 Flowability 27
4.1.2 Compressive Strength 32
4.1.3 Modulus of Elasticity 47
4.1.4 Splitting Tensile Strength 49
4.1.5 Flexural Strength/Modulus of Rupture 54
4.1.6 Freeze-Thaw Mix 65
4.2 Florida International University (FIU) Materials J3 Mix 77
4.2.1 Flowability 77
4.1.2 Compressive Strength 81
4.1.3 Flexural Strength/Modulus of Rupture 89
Chapter 5: Summary, Conclusions, and Recommendations 106
5.1 Summary 106
5.2 Conclusions 106
5.3 Recommendations 109
References 111
Appendix A: Compressive Strength Specimens 113
Appendix B: Constituent Material Information 118
Appendix C: Individual Specimen Data 119

List of Tables

Table 1: J3 testing matrix 12

Table 2: Mix design of J3 for various percentages of fibers 13

Table 3: OU J3 flow test results 27

Table 4: OU J3 cylinder compressive strength test data for each steel fiber content 32

Table 5: OU J3 cube compressive strength test data for each steel fiber content 34

Table 6: OU J3 modulus of elasticity data 47

Table 7: OU J3 splitting tensile strength test results 50

Table 8: OU J3 flexural strength (MOR) for each steel fiber content 54

Table 9: Freeze-thaw flow test results 65

Table 10: Freeze-thaw vs. OU J3 28 day cylinder compressive strength test results for each steel fiber content 66

Table 11: FIU J3 flow test results 78

Table 12: FIU J3 cylinder compressive strength test data for each steel fiber content 81

Table 13: FIU J3 cube compressive strength test data for each steel fiber content 82

Table 14:Comparison of OU J3, Freeze-thaw, and FIU J3 28 day cylinder compressive strength test results for each fiber content 84

Table 15: OU J3 vs. FIU J3 flexural strength (MOR) for each steel fiber content 90

Table 16: OU J3 and FIU J3 mix component information 118

Table 17: OU J3 and FIU J3 compressive strength (psi) for each individual cylinder specimen for each steel fiber content 119

Table 18: OU J3 splitting tensile strength (psi) for each individual specimen for each steel fiber content 120

Table 19: OU J3 and FIU J3 flexural strength (MOR) (psi) for each individual specimen for each steel fiber content 121

List of Figures

Figure 1: Smaller batch of UHPC in mixer 13

Figure 2: Steel fibers being added during mixing..... 14

Figure 3: Batch of J3 specimens immediately after casting 15

Figure 4: Specimens curing in tank 15

Figure 5: Standard flow test set up 17

Figure 6: Standard compressive strength test set up for cube (left) and cylinder (right) specimens 18

Figure 7: Standard MOE test set up..... 20

Figure 8: Standard splitting tensile strength test set up 21

Figure 9: Standard MOR test set up..... 23

Figure 10: James Instruments E-Meter device used to record resonant frequency data during the freeze-thaw test 25

Figure 11: Freeze-thaw test specimen set up set up to measure resonant frequency..... 25

Figure 12: Metal ball and distance of hit used to determine resonant frequency for the freeze-thaw tests..... 26

Figure 13: Freeze-thaw specimens in the freeze-thaw chamber..... 26

Figure 14: OU J3 0% fiber mix flow test..... 29

Figure 15: OU J3 1% fiber mix flow test..... 29

Figure 16: OU J3 2% fiber mix flow test..... 30

Figure 17: OU J3 4% fiber mix flow test..... 30

Figure 18: OU J3 6% fiber mix flow test..... 31

Figure 19: OU J3 6% mixture immediately after mixing 31

Figure 20: OU J3 cylinder compressive strength test results..... 33
Figure 21: OU J3 cube compressive strength test results 35
Figure 22: OU J3 0% cylinder 3 day compressive strength test specimens after failure..... 37
Figure 23: OU J3 0% cylinder 7 day compressive strength test specimens after failure..... 37
Figure 24: OU J3 0% cylinder 28 day compressive strength test specimens after failure..... 38
Figure 25: OU J3 0% cylinder 56 day compressive strength test specimens after failure..... 38
Figure 26: OU J3 0% cube 28 day compressive strength test specimens after failure 39
Figure 27: OU J3 1% cylinder 28 day compressive strength test specimens after failure..... 39
Figure 28: OU J3 1% cube 56 day compressive strength test specimens after failure 40
Figure 29: OU J3 2% cylinder 28 day compressive strength test specimens after failure..... 40
Figure 30: OU J3 2% cylinder 56 day compressive strength test specimens after failure..... 41
Figure 31: OU J3 2% cube 28 day compressive strength test specimens after failure 41
Figure 32: OU J3 2% cube 56 day compressive strength test specimens after failure 42
Figure 33: OU J3 4% cylinder 28 day compressive strength test specimens after failure..... 42
Figure 34: OU J3 4% cylinder 56 day compressive strength test specimens after failure..... 43
Figure 35: OU J3 4% cube 28 day compressive strength test specimens after failure 43
Figure 36: OU J3 4% cube 56 day compressive strength test specimens after failure 44
Figure 37: OU J3 6% cylinder 3 day compressive strength test specimens after failure..... 44
Figure 38: OU J3 6% cylinder 28 day compressive strength test specimens after failure..... 45
Figure 39: OU J3 6% cylinder 56 day compressive strength test specimens after failure..... 45
Figure 40: OU J3 6% cube 3 day compressive strength test specimens after failure 46
Figure 41: OU J3 6% cube 28 day compressive strength test specimens after failure 46
Figure 42: OU J3 6% cube 56 day compressive strength test specimens after failure 47

Figure 43: OU J3 MOE results 49
Figure 44: OU J3 split cylinder test 50
Figure 45: OU J3 0% 28 day splitting tensile test specimens after failure 51
Figure 46: OU J3 1% 28 day splitting tensile test specimens after failure 52
Figure 47: OU J3 2% 28 day splitting tensile test specimens after failure 52
Figure 48: OU J3 4% 28 day splitting tensile test specimens after failure 53
Figure 49: OU J3 6% 28 day splitting tensile test specimens after failure 53
Figure 50: OU J3 MOR maximum load at 28 and 56 days 55
Figure 51: OU J3 MOR results normalized by square root of compressive strength 57
Figure 52: OU J3 0% 28 day MOR test specimens after failure 60
Figure 53: OU J3 1% 28 day MOR test specimens after failure 60
Figure 54: OU J3 2% 28 day MOR test specimens after failure 61
Figure 55: OU J3 4% 28 day MOR test specimens after failure 61
Figure 56: OU J3 6% 28 day MOR test specimens after failure 62
Figure 57: OU J3 0% 56 day MOR test specimens after failure 62
Figure 58: OU J3 1% 56 day MOR test specimens after failure 63
Figure 59: OU J3 2% 56 day MOR test specimens after failure 63
Figure 60: OU J3 4% 56 day MOR test specimens after failure 64
Figure 61: OU J3 6% 56 day MOR test specimens after failure 64
Figure 62:OU J3 (left) vs. freeze-thaw J3 (right) 6% fiber mix flow test 66
Figure 63: Freeze-thaw vs. OU J3 28 day cylinder compressive strength test results..... 67
Figure 64: Freeze-thaw 0% 28 day cylinder compressive strength test specimens after failure .. 68
Figure 65: Freeze-thaw 1% 28 day cylinder compressive strength test specimens after failure .. 69

Figure 66: Freeze-thaw 2% 28 day cylinder compressive strength test specimens after failure .. 69
Figure 67: Freeze-thaw 4% 28 day cylinder compressive strength test specimens after failure .. 70
Figure 68: Freeze-thaw 6% 28 day cylinder compressive strength test specimens after failure .. 70
Figure 69: Freeze-thaw progression of average frequency over time..... 71
Figure 70: Freeze-thaw progression of relative dynamic modulus over time 72
Figure 71: Freeze-thaw specimens after 0 cycles (07/01) 73
Figure 72: Freeze-thaw specimens after 351 cycles (11/03 final day) 73
Figure 73: Close up view of freeze-thaw specimen ends after 351 cycles (11/03 final day) 74
Figure 74: Freeze-thaw specimens after 351 cycles (11/03 final day) showing rusted exposed fibers 74
Figure 75: Freeze-thaw first sign of rust on 2% specimen after 9 cycles (07/08) 75
Figure 76: Freeze-thaw 6% specimens after 0 (7/01) (left), 42 (7/15) (middle), and 351 cycles (11/03) (right)..... 76
Figure 77: Freeze-thaw chamber trays after 351 cycles (11/03 final day) 77
Figure 78: FIU J3 0% fiber mix flow test 79
Figure 79: FIU J3 1% fiber mix flow test 79
Figure 80: FIU J3 4% fiber mix flow test 80
Figure 81: FIU J3 6% fiber mix flow test 80
Figure 82: FIU J3 cylinder compressive strength test results 82
Figure 83: FIU J3 cube compressive strength test results..... 83
Figure 84: Comparison of OU J3, Freeze-thaw, and FIU J3 28 day cylinder compressive strength test results..... 84
Figure 85: OU J3 vs. FIU J3 56 day cylinder compressive strength test results 85

Figure 86: OU J3 vs. FIU J3 28 day cube compressive strength test results 85
Figure 87: OU J3 vs. FIU J3 56 day cube compressive strength test results 86
Figure 88: FIU J3 0% cylinder 28 day compressive strength test specimens after failure 87
Figure 89: FIU J3 1% cylinder 28 day compressive strength test specimens after failure 87
Figure 90: FIU J3 2% cylinder 28 day compressive strength test specimens after failure 88
Figure 91: FIU J3 4% cylinder 28 day compressive strength test specimens after failure 88
Figure 92: FIU J3 6% cylinder 28 day compressive strength test specimens after failure 89
Figure 93: FIU J3 MOR maximum strength 28 vs 56 day 91
Figure 94: OU vs. FIU J3 MOR results at 28 days and 56 days 92
Figure 95: OU vs. FIU J3 MOR results at 28 days 92
Figure 96: OU vs. FIU J3 MOR results at 56 days 93
Figure 97: FIU J3 MOR results normalized by square root of compressive strength 93
Figure 98: OU and FIU J3 MOR results normalized by square root of compressive strength for 28 and 56 days 94
Figure 99: FIU J3 0% 28 day MOR test specimens after failure 96
Figure 100: FIU J3 0% 28 day MOR test specimen cross section 96
Figure 101: FIU J3 1% 28 day MOR test specimens after failure 97
Figure 102: FIU J3 2% 28 day MOR test specimens after failure 97
Figure 103: FIU J3 4% 28 day MOR test specimens after failure 98
Figure 104: FIU J3 6% 28 day MOR test specimens after failure 98
Figure 105: FIU J3 0% 56 day MOR test specimens after failure 99
Figure 106: FIU J3 1% 56 day MOR test specimens after failure 99
Figure 107: FIU J3 2% 56 day MOR test specimens after failure 100

Figure 108: FIU J3 4% 56 day MOR test specimens after failure 100
Figure 109: FIU J3 6% 56 day MOR test specimens after failure 101
Figure 109: FIU J3 0% 28 day MOR test load vs. deflection curve 102
Figure 109: FIU J3 1% 28 day MOR test load vs. deflection curve 103
Figure 112: FIU J3 2% 28 day MOR test load vs. deflection curve 103
Figure 113: FIU J3 4% 28 day MOR test load vs. deflection curve 104
Figure 114: FIU J3 6% 28 day MOR test load vs. deflection curve 104
Figure 115: FIU J3 28 day test load vs. deflection curve for all fiber percentages 105
Figure 116: OU J3 0% cube 3 day compressive strength test specimens after failure 113
Figure 117: OU J3 0% cube 56 day compressive strength test specimens after failure 113
Figure 118: OU J3 1% cylinder 3 day compressive strength test specimens after failure..... 114
Figure 119: OU J3 1% cylinder 7 day compressive strength test specimens after failure..... 114
Figure 120: OU J3 1% cylinder 56 day compressive strength test specimens after failure..... 115
Figure 121: OU J3 1% cube 3 day compressive strength test specimens after failure 115
Figure 122: OU J3 2% cylinder 3 day compressive strength test specimens after failure..... 116
Figure 123: OU J3 2% cylinder 7 day compressive strength test specimens after failure..... 116
Figure 124: OU J3 2% cube 3 day compressive strength test specimens after failure 117

Abstract

Ultra-high performance concrete (UHPC) is an extremely durable type of concrete that includes high volumes of cementitious material, fine aggregate, superplasticizer, and steel fibers with an overall low water to cement ratio and has mechanical properties that significantly exceed those of typical concrete. Researchers at the University of Oklahoma (OU) have developed a non-proprietary version of UHPC using materials available locally in Oklahoma under the name of J3 with properties similar to commercially available UHPC mixes. While all other ratios of materials in the mix have been established, the effect of different percentages of steel fibers on material properties were yet to be tested. The research described in this thesis includes varying the steel fiber concentration within the mix to identify how different amounts of fibers – more specifically 0, 1, 2, 4, and 6% – affect flow, compression, and tension properties of this non-proprietary UHPC mix. The goal of this research was to determine which percentage of fibers resulted in the best performance and identify the best concentration of steel fibers for a particular structural application. This was done by putting specimens with each percentage of fibers through rigorous testing including flow, compressive strength, modulus of elasticity, splitting tensile strength, flexural strength, and freeze-thaw.

Another objective of this study was to determine if it would be plausible to recreate the performance of the OU J3 mix even when using materials from other locations. The mix was recreated using sand, slag, and cement from sources available locally in Florida and provided by collaborators at Florida International University (FIU) who were partners for this phase of the research. Flow, compressive strength, and flexural strength were tested for specimens cast from this mix of J3.

The results of the research suggest that for both material locations increasing the percentage of steel fibers increases compressive and tensile strength with diminishing returns for higher fiber contents. Of those tested, the optimal mix for most applications would contain 2% steel fibers by volume, while for extreme cases where additional compressive or tension strength is required higher percentages could be used. The results also revealed that while there was an increase in strength between the material properties at 28 and 56 days of age, this difference decreased with increase in fibers. Additionally, both the OU J3 and FIU J3 mixes behaved similarly for all tests performed indicating that the mix design is repeatable using materials from other sources.

Chapter 1: Introduction

Ultra-High Performance Concrete (UHPC) is a recently developed type of cementitious material that has fresh, mechanical, and durability properties unlike and far exceeding those of conventional concrete. "UHPC in its present form started to become commercially available in North America by the late 1990s; first in Canada in the late 1990s followed by the US in the early 2000s" (Haber, 2018). The most notable attribute of UHPC is that it is "composed of a very dense cementitious matrix with a discontinuous pore structure that results in very low permeability and high compressive strength. Furthermore, the matrix is reinforced with high volumes (typically equal to or greater than 2 percent fiber by volume) of high-strength steel microfiber reinforcement which allows for post-cracking tensile ductility" (Haber, 2018). It must be noted that definitions of strength of UHPC vary and there is not a single fully established one, but the Federal Highway Administration (FHWA) defines UHPC as "a cementitious composite material composed of an optimized gradation of granular constituents, a water-to-cementitious materials ratio less than 0.25, and a high percentage of discontinuous internal fiber reinforcement. The mechanical properties of UHPC, as defined by FHWA, include compressive strength greater than 21.7 ksi (150 MPa) and sustained postcracking tensile strength greater than 0.72 ksi (5 MPa)" (FHWA, 2018). UHPC has been successfully used to connect precast concrete slabs and bridge components, which is possible due to its superior bond development characteristics with steel reinforcement, ease of placement, and long-term durability as compared to conventional concrete (Graybeal, 2010). Use as a connection material has been one of the more popular recent UHPC applications, but these unique mechanical properties also allow for the optimization of structural elements, such as bridge girders, where the enhanced tensile strength can help eliminate the need for mild steel shear reinforcement (Graybeal, 2006). UHPC

is also often considered for bridge rehabilitation solutions such as overlays, link slabs to rehabilitate deteriorated expansion joints, encasement to rehabilitate deteriorated steel beams at leaking joints, and pile/column jacketing (Haber, 2018). In most of these applications a smaller quantity of UHPC is required to complete the project or the repair than the volume of conventional concrete that would be required to achieve a similar strength.

The benefits of using UHPC for a wide variety of applications are evident, but the currently commercially available proprietary mixtures are very expensive. The most widely used UHPC material in the United States is a proprietary mix sold under the trademark Ductal®, produced by LafargeHolcim Ltd. This mix has typically been used in previous research projects as the UHPC material, however, Ductal® currently costs around $3000 per cubic yard, which is about 20 times the cost of conventional concrete due to its high cementitious materials content and fiber reinforcement (Waidelich, 2014). UHPC mixes can be made with local materials in order to reduce costs. Several state Departments of Transportation have sponsored research in the past, are currently researching the possibility of developing non-proprietary mixes, or are evaluating more cost effective UHPC materials developed by others (Waidelich, 2014). Exact compositions of UHPC may vary among products, but the mix design components are generally very similar. UHPC typically consists of dry components, such as cement, silica fume, and fine aggregates; chemical admixtures, such as accelerators and high range water reducers (HRWR); water; and steel fibers. The mix design being considered in this study was developed as part of previous research (Looney et al., 2019) and consists of Type I portland cement, slag cement, silica fume, water, fine masonry sand, steel fibers, and MasterGlenium 7920 high-range water reducer (HRWR) with a 0.2 water-cementitious materials ratio.

The first objective of the study was to evaluate the effect of various volumetric portions of steel fibers on the properties of a developed and previously tested non-proprietary UHPC mix. Typically, steel fibers are used in UHPC in order to prevent brittle failure because they help the concrete retain flexural strength after cracking. Tensile strength capacity also greatly increases due to fibers. Adding steel fibers to UHPC can have a great impact on its properties and may alter the crack patterns, delay the crack appearance, and restrain the crack expansion in concrete specimens (Shehab El-Din, 2016). However, steel fibers are most expensive component of the mix design. The research described in this thesis included varying the steel fiber concentration within the mix to identify how different amounts of steel fibers affect flow, compression, and tension properties of non-proprietary UHPC mix, determine which percentage of fibers resulted in the best performance, and identify the best concentration of steel fibers for a particular structural use. Optimizing the steel fiber content for a given application would help streamline the future design and usage of UHPC on various projects and potentially reduce cost, especially if a smaller amount of steel fibers is needed to achieve the same behavior under particular conditions. The second objective of this study was to identify the effects of materials from different areas of the country on flow, compressive strength, and tension properties of the baseline UHPC mix in order to better understand how to adapt a given UHPC mix to different local materials. This could make UHPC more easily accessible by using local materials and thus further reduce cost and ability to incorporate it in more projects across the country.

Chapter 2: Literature Review

2.1 Defining Ultra-High Performance Concrete

Ultra-high performance concrete (UHPC) is a cementitious, concrete material that has a much higher compressive strength, durability, tensile ductility, and toughness than a typical concrete mix (Portland Cement Association, 2019). As previously stated, definitions of UHPC vary depending on the source, but in general its 28-day specified compressive strength should be higher than 17,000 psi (120 MPa). UHPC can be formulated to provide compressive strengths in excess of 29,000 psi (200 MPa), and, when combined with metal fibers, it can achieve flexural strengths up to 7,000 psi (48 MPa) or greater (PCA). UHPC is typically made with a high content of cementitious materials, fine aggregate, superplasticizer, and steel fibers with an overall low water-cementitious materials ratio (Wu et al., 2015). The low water-cementitious materials ratio leads to the high compressive strength and an optimized particle gradation contributes to flowability and mixture density, which directly relates to durability.

While the mixture lacks any coarse aggregate, it is the steel fibers that are truly unique and are generally included in the mixture to achieve superior mechanical properties, especially flexural and bond strength. The use of steel fibers "can provide UHPC with strain-hardening behavior in tension and transform the brittle failure to ductile failure" (Wu et al., 2015). Unfortunately, with higher strength, comes higher cost. "Use of UHPC in the United States has been limited due to the lack of domestic production capacity of the steel fiber reinforcement that is used in the UHPC mix" (Waidelich, 2014). As of 2014, there was only one manufacturer of UHPC in the United States –LafargeHolcim Ltd with their proprietary mix under the trademark of Ductal®, and only a very limited number of manufacturers have joined the market since 2014. This limited availability and trademark make the use of UHPC, while very effective, also very

expensive. Over last few years “some State DOTs are working with academia to develop non-proprietary mix designs that meet the performance requirements similar to those provided by UHPC” (Waidelich, 2014) with the University of Oklahoma (OU) being one of these institutions. While the whole matrix composition (such as the cement types and quantities as well as the overall gradation of the cementitious and aggregate constituents) has a huge effect on the flow and compressive properties, the steel fibers are also a very important aspect of the mix.

2.2 Steel Fibers in UHPC

Previous research into effects of steel fibers on mechanical properties of UHPC has revealed that different variations of fiber content by volume (V_f = 0, 1, 2, and 3 percent) and shape of steel fibers (straight, corrugated, and hooked-end) cause considerable change to the properties of the mix (Wu et al., 2015). “The results indicated that increased fiber content and use of deformed fibers could gradually decrease the flowability of UHPC. They also had significant effects on compressive and flexural behavior of UHPC” (Wu et al., 2015). According to the research of Wu et al. (2015), “steel fiber content had limited effect on the first crack strength and first crack deflection of flexural load–deflection curve of UHPC but showed considerable effects on the peak load.” In this paper (Wu et al. (2015)), the type of UHPC used was not specified (proprietary or non-proprietary), but based on the topic of the research and the ingredients described, it can be assumed that this was an already existing, previously tested mix to isolate the steel fibers as the only variable of the experiment. Another study by Hoang and Fehling (2017) looked into the “effect of steel fiber contents of 1.5% and 3% with different aspect ratios on the uniaxial tensile and compressive behavior of UHPC.” The study used M3Q, a UHPC mixture that was developed at the University of Kassel in Germany (Hoang and Fehling, 2017). They found that “there is no noticeable change in the compressive strength and

elastic modulus with incorporation of steel fibers, however the postpeak behavior under compression is substantially affected by steel fiber content and aspect ratio. In terms of notched prisms under tension, they found no influence of steel fiber in the linear elastic stage, whereas the increase in steel fiber content resulted in not only a significant effect on the fiber activation stage but also higher values of fiber efficiency" (Hoang and Fehling, 2017).

2.3 Non-Proprietary UHPC Mixes

With so few sources of UHPC, "the vast majority of field usage of UHPC in the US, to date, has employed pre-packaged, proprietary materials" (El-Tawil et al., 2018). There have been several efforts to develop a generic, cost-optimized UHPC mix, among them a previous project funded by Michigan DOT, which developed a UHPC mix design (named MI-UHPC) "that performed exceptionally well in the lab but was not well suited for field implementation" (El-Tawil et al., 2018). Previously UHPC has been used mostly for bridge repair and construction. It is hoped that further research into this topic "will spur commercial production and utilization of non-proprietary UHPC and broaden its appeal and range of application" (El-Tawil et al., 2018). At this point, it is known that "generic UHPC can be successfully mixed using components sourced from a variety of suppliers as long as a proper high-range water reducer (HRWR) dose is selected" (El-Tawil et al., 2018). "Too low of a dose will prevent the mix from turning over" and mixing properly (El-Tawil et al., 2018). "Increasing the HRWR dose can lead to mildly reduced mechanical properties, but does not compromise the long term properties of UHPC. Too high of a dose can lead to fiber segregation, which is undesirable and should be avoided" (El-Tawil et al., 2018).

Typically, a final standard non-proprietary UHPC mixture achieves a compressive strength of at least 22 ksi (150 MPa) and maintains self-consolidation properties (El-Tawil et al.,

2016). This strength is required by the FHWA definition, but other UHPC class materials could be developed that do not meet this compressive strength requirement, yet still exhibit similar structural performance. Among the efforts to develop a non-proprietary blend and to reduce the cost of UHPC, a study was conducted in 2016 by El-Tawil et al. that took a closer look at the most expensive ingredients within the mix besides the steel fibers – cement, silica fume and silica powder. By adjusting the type and amount of these ingredients, several batches were cast and "short-term material performance was assessed via tensile and compressive tests" while "durability properties were evaluated based on freeze-thaw and chloride ion penetration testing as well as quantification of the presence and distribution of air voids" (El-Tawil et al. 2016). "The test results were used to optimize cost versus performance characteristics of the UHPC blends considered" (El-Tawil et al. 2016). The final mix that yielded the best results uses a "50:50 mix of Portland Type I and Ground Granulated Blast Furnace Slag (GGBFS) as a binder, lacks any Silica Powder (inert filler) and requires no post-placing treatment", in which it greatly deviates from traditional UHPC mixtures (El-Tawil et al. 2016). By exploring this new mix, "the cost of the cementitious material ingredients was reduced by half compared to available non-proprietary UHPCs available at the onset of this research" (El-Tawil et al. 2016). It must be noted that because there is no set non-proprietary UHPC formula at this time, the results of different studies will vary depending on the specific mix the researchers choose to analyze and the properties they want to improve.

Although the formula developed by El-Tawil et al. in 2016 was the focus of further research conducted by El-Tawil et al. in 2018 into further analysis of the behavior of this non-proprietary mix in the lab and in the field, one important aspect of a non-proprietary mix is its availability regardless of location. Thus, in order to ensure that the non-proprietary UHPC

investigated in the study by El-Tawil et al. in 2018 was truly generic, its components were sourced from multiple vendors. “In particular, the ordinary portland Type I cement, silica fume, and high range water reducer used in this research were each obtained from three different suppliers to study the effect of material sources on UHPC performance” (El-Tawil et al., 2018). Even a small variation in the size of aggregate can cause the mix to have different properties than intended, but this can be adjusted by using the appropriate amount of HRWR. However, the amount of HRWR should stay between 1.5-3 percent by weight of cement to avoid adverse effects (El-Tawil et al., 2018).

In regards to the steel fibers within this non-proprietary mix, “the test data showed that the aspect ratio of the steel fibers seems to play a relatively minor role in the compressive strength of UPHC. However, a higher aspect ratio is beneficial for redistribution of stresses after first cracking under tensile load and promotes multiple crack development, which enhances energy absorption characteristics” (El-Tawil et al., 2018). While this study mostly focused on testing the effects of two different aspect ratios of steel fibers (as well as the effects of short and long steel fibers) and investigated the possibility of replacing steel fibers with polyethylene fibers, the authors determined that “reducing the steel fiber volume fraction from 2% to 1.5% also has a mild effect on the compressive strength (a 5% reduction was observed)” (El-Tawil et al., 2018).

Along with other universities, researchers at the University of Oklahoma (OU) conducted studies into the properties of proprietary and non-proprietary UHPC in order to reduce the costs of this material. Through various tests involving many variations of the mix, it was determined that the main driver of compressive strength was the “chemical composition of mix constituents” (Looney et al., 2019). Among the factors with the largest effects on the mix was using Type II

cement, which “appeared to improve the flow of mixes at higher quantities due to its lower water demand” (Looney et al., 2019). Another observation was that mixes with GGBFS and portland cement “were able to perform better than similar mixes with only cement” (Looney et al., 2019). From these observations and further testing, it was determined that the third mix in series J (J3) was the best performing mixture (Looney et al. 2019). J3 has properties very similar to commercially available UHPC and it has become the focus of OU’s non-proprietary UHPC research, including the study described in this thesis.

2.4 Existing Issues with Non-Proprietary UHPC

In the past research there were four significant issues encountered when trying to mix non-proprietary UHPC on site in the field, these included: “1) the silica fume used in the field had a high carbon content, which drove up water demand, 2) the dosage of the high range water reducer (HRWR) was too low to compensate for the higher water demand, making mixing more difficult, 3) the silica fume was a densified product that posed an additional challenge for the mixer as it tried to deagglomerate the material and sufficiently disperse it during dry mixing, and 4) the field mixer did not have sufficient capacity to induce turnover in the wet mix, compromising the mixing process” (El-Tawil et al., 2018). These factors should still be considered when mixing in a lab setting as well because any small variation in the ingredients or mixing procedure can cause an alteration to the final product.

2.5 Summary

The non-proprietary mix developed by El-Tawil et al. (2016) shows great promise and is currently being developed and tested even further in a variety of ways, but the effects of each of its components in different proportions has yet to be extensively explored, especially when it comes to the steel fibers that drastically increase the tensile strength, ductility, and energy

dissipation capacity. These effects greatly depend on the physical properties of the fibers themselves, and on the concentration of fibers within the mix. This latter aspect is yet to be explored in the context of the non-proprietary mix described above in detail. Additionally, it is evident from the Wu et al. (2015) and Hoang and Fehling (2017) studies that a percent by volume of fibers above three percent has not been studied to the same extent as the amounts under three percent.

Even with the results of these previous studies, it seems that there has not been a study that comprehensively examined UHPC properties (flowability, compressive strength, modulus of elasticity and Poisson's ratio, splitting tensile strength, flexural strength, direct tension, total shrinkage, compressive creep, setting time, freeze-thaw resistance, rapid chloride ion permeability, and drying shrinkage) on a wider variety of percent fibers by volume, especially in the higher range above three percent. Thus with all the available research on UHPC, while all of the other materials in the mix have been established, it is still mostly unknown what effect different volumes of steel fibers have on mechanical properties of non-proprietary UHPC, which is the focus of the research described in this thesis.

Lastly as described in an earlier section, a potential challenge of using non-proprietary UHPC in the field is the variation in properties due to use of the same required materials but from different sources or locations across the country. This potential variability is explored in this thesis by comparing an analyzing the mechanical properties of a UHPC mix developed at OU under the name of J3 (Looney et al. 2019) by using two different sources for the sand, slag, and cement and comparing the flow, compressive strength, and flexural strength.

Chapter 3: Approach and Methods

3.1 Overview

The experimental investigation conducted in this project consisted of two parts. For the initial set of tests examining the effect of steel fiber content on the non-proprietary J3 UHPC mix design developed at OU, a total of five 2.5 ft^3 batches were cast and tested each with a different percentage by volume of steel fibers. These fiber contents were 0, 1, 2, 4, and 6% and the fibers that were used are Dramix® OL 13/0.20 fibers manufactured by Bekaert. They are 0.5 in. long, have 0.0079 in. diameter, and are rated at 313 ksi. Specimens cast from these mixes were tested at 3, 7, 28, and 56 days for compressive strength, 28 days for modulus of elasticity (MOE) and splitting tensile strength, and 28 as well as 56 days for the flexural strength (modulus of rupture (MOR)). A flowability test was conducted as soon as the batch had been mixed. The only variable adjusted for each batch was the steel fiber content, however this affected the amounts of other materials required to maintain a constant volume of the total mix. Each other constituent was decreased proportionally to the increase in steel fibers. The amount of high range water reducer (HRWR) also had to be increased for the 4 and 6% steel fiber mixes in order to achieve the required workability of the concrete mixture. In addition to the mechanical property tests, a batch with each percentage of fibers was mixed to cast specimens for the freeze-thaw test, which was run for 350 cycles starting at 14 days of age. Three compression cylinders were cast for each fiber percentage out of the same batch of concrete as the freeze-thaw specimens and tested at 28 days.

Furthermore, to assess if a given non-proprietary UHPC mix can be recreated from different local materials, a batch with each fiber percentage was mixed using the cement, slag, and sand locally available in the Miami, Florida area provided by researchers at Florida

International University (FIU). For these mixes, compressive strength tests were performed at 3, 7, 28, and 56 days; modulus of rupture tests were performed at 28 and 56 days; and flow tests were performed the day of each pour. Table 1 is a testing matrix for each of the three mix types described above that further details which tests were performed on which days. All testing was performed at the Donald G. Fears Structural Engineering Laboratory on the University of Oklahoma campus.

Table 1: J3 testing matrix

Concrete Age (Days)	**OU J3**	**Freeze-thaw J3**	**FIU J3**
0	flow	flow	flow
3	compression	__	compression
7	compression (cylinders only)	__	compression
28	compression split cylinder MOE MOR	compression	compression MOR
56	compression MOR	__	compression MOR

3.2 Mixing Procedure

The proportions used for the J3 mixes examined in this study are listed in Table 2 (additional properties and manufacturers of the constituent materials are listed in Table 16 in Appendix B). The mixture was designed to have a 0.2 water to cement ratio. Each batch was mixed by first weighing out and combining all the dry materials and mixing them together using a high-shear mechanical mixer for 10 minutes. With the mixer still running, half of the HRWR was added into the required water and this mixture was added to the main mixture over the course of 2 minutes (from 10 to 12 minutes). The mixer was then run for 1 minute (from 12 to 13

minutes) and the remainder of the HRWR was added over the course of 1 minute with the final time being 14 minutes. The UHPC mixture was then allowed to mix for an additional 9 to 10 minutes or until it obtained a liquid consistency. Figure 1 shows the mixer and mix during this part of the mixing process. If applicable, at this time the steel fibers were added into the mixture, as shown in Figure 2, and the mixer was run for an additional 2 minutes before discharging.

Table 2: Mix design of J3 for various percentages of fibers

Mix Series	**Material**	**% Fibers (by volume)**				
		0	**1**	**2**	**4**	**6**
OU & FIU	Type I Cement [lb/yd^3]	1203.7	1191.6	1179.6	1155.5	1131.4
	Slag [lb/yd^3]	601.8	595.8	589.8	577.8	565.7
	Silica Fume [lb/yd^3]	200.6	198.6	196.6	192.6	188.6
	Water [lb/yd^3]	401.22	397.2	393.2	385.18	377.14
	Fine Masonry Sand [lb/yd^3]	2006.1	1986	1966	1925.9	1885.7
	Steel Fibers [lb/yd^3]	0.0	132.3	264.5	529	793.5
OU	Glenium 7920 [oz./cwt]	18	18	18	23	28
	Glenium 7920 [oz/yd^3]	361.1	357.5	353.9	443.0	528.0
FIU	Glenium 7920 [oz./cwt]	23	23	23	25	30
	Glenium 7920 [oz/yd^3]	461.4	456.8	452.2	481.5	565.7



Figure 1: Smaller batch of UHPC in mixer



Figure 2: Steel fibers being added during mixing

The mixer shown in Figure 1 and 2 was used for the freeze-thaw (0.5 ft^3) and FIU J3 (0.075 ft^3) batches, while for the OU J3 (2.5 ft^3) batch a Mixer Systems, Inc. 21 DD horizontal shaft mixer was used.

3.3 Specimen Curing

Upon completion of mixing, the concrete was promptly poured into specimen molds that were primed with form release oil. Figure 3 shows specimen molds immediately after casting. The filled molds were covered with plastic and left to cure for 3 days in a controlled environment in a room with temperature at 73.5 ± 3.5°F (23.0 ± 2.0°C) and approximately 50 percent relative humidity. At the end of 3 days some specimens were taken for testing while the rest were demolded and placed in a tank filled with water and lime within the environmentally controlled room for further curing, as shown in Figure 4. Each specimen remained in the tank until the day of testing.



Figure 3: Batch of J3 specimens immediately after casting



Figure 4: Specimens curing in tank

3.4 Specimen Testing

Each of the following standard tests was performed for each of the five steel fiber content variations of the OU J3 non-proprietary UHPC mix. Modifications to the standard test methods were made according to ASTM C1856 (2017) for testing UHPC and as described below. For the specimens cast with materials from FIU only the flow, compressive strength, and MOR tests were performed. The number of specimens given are the amounts used for one batch for one fiber content.

3.4.1 Flowability

The flowability test was performed as soon as possible after the mixing was finished in accordance with ASTM C1437 – *Standard Test Method for Flow of Hydraulic Cement Mortar (2015)* modified according to ASTM C1856 (2017). As soon as the mixing stopped a sample of the mixture was taken over to the flow table and placed into the metal mold. A timer was then started for 2 minutes and the mold taken off. The mixture was left undisturbed and allowed to flow (as shown in Figure 5). At the end of 2 minutes the diameter of the flow was measured at multiple spots across the flow table and the average of the diameters recorded. The desired flow was greater than or equal to 8 in. If the appropriate flow was not achieved using the standard amount of HRWR, then the amount of HRWR was increased until sufficient flow was reached, which was required for the 4 and 6% mixes for OU J3 and for all fiber percent mixes for FIU J3. Prior to determining the final amount of HRWR to be used in all mixes, several small batches were made to ensure the proper amount for the final casting. The 4 and 6% mixes were the ones most heavily impacted for both the OU J3 and FIU mixes. It was determined that the amount of HRWR would need to be increased for those two fiber contents based on how the 2% batch behaved. Several trials were run by altering the amount of HRWR each time, however the 8 in.

flow requirement was not plausible with the 6% fiber content without causing significant segregation of the fibers from the rest of the mixture. In this case workability of the concrete was considered adequate with a lower flow; the flow had to only be enough to properly put the mix into the molds.



Figure 5: Standard flow test set up

3.4.2 Compressive Strength

The compressive strength testing for this research was performed on 2 in. by 2 in. cubes as well as 3 in. by 6 in. cylinders. Testing was done in accordance with ASTM C39/C39M – *Standard Test Methods for Compressive Strength of Cylindrical Concrete Specimens (2018)* and *C109/C109M – Standard Test Method for Compressive Strength of Hydraulic Cement Mortars (Using 2-in. or [50-mm] Cube Specimens) (2020)* with the modifications listed in ASTM C1856 (2017), using the Forney compression machine at Fears Lab. Figure 6 shows how cube and cylinder samples were loaded into the Forney machine. For the OU J3 mix 9 cubes and 12

cylinders were cast for each fiber content and for the FIU mix 12 cubes and 12 cylinders were cast. Three of each specimen type were tested at 3, 7, 28, and 56 days except for the OU J3 cube 7 day testing was omitted. From the freeze-thaw batch 3 cylinders were cast to be tested at 28 days. Because of the higher strength of UHPC the compression loading rate for all specimens was adjusted to 150 psi/s as specified in ASTM C1856 (2017). All cylinders were ground plane to the ASTM C39 specification using a cylinder end grinder before testing.



Figure 6: Standard compressive strength test set up for cube (left) and cylinder (right) specimens

3.4.3 Modulus of Elasticity

The modulus of elasticity (MOE) testing for this research was performed on 4 in. by 8 in. cylinders. Testing was done in accordance with ASTM C469/C469M – *Standard Test Method for Static Modulus of Elasticity and Poisson's Ratio of Concrete in Compression (2014)* with the load rate adjusted to 150 psi/s as specified in *ASTM C1856 (2017)*. Prior to testing the cylinders were ground plane using a cylinder end grinder. Then, as depicted in the left picture in Figure 7, the cylinder was placed precisely in the center of the compressometer and secured in place, ensuring sufficient and equal spacing from the bottom and the top. A linear voltage differential transformer (LVDT) was also attached to the compressometer to measure longitudinal deformation that could be converted to strain. It was attached to the compressometer in a way that the LVDT was almost fully extended. The cylinder was then placed into the Forney machine (Figure 7 right image) and each specimen one was loaded to a load equal to 40% of the compressive strength, which was calculated based on the dimensions of the sample as well as the average of the compressive strengths of the cylinders (unless the compression data from the cylinders was suspect, then results from the cubes were used). Each cylinder was loaded three times and the data from the first run for each specimen was discarded. For the J3 mix with each fiber percentage 3 cylinders were cast and tested at 28 days. From the data collected the modulus of elasticity was calculated using the Equation 1.

$$E = (S_2 - S_1)/(\varepsilon_2 - 0.000050) \quad (1)$$

Where E = chord modulus of elasticity (psi), S_2 = stress corresponding to 40% of ultimate load (psi), S_1 = stress corresponding to a longitudinal strain, ε_1, of 50 millionths (psi), and ε_2 = longitudinal strain corresponding to stress S_2.

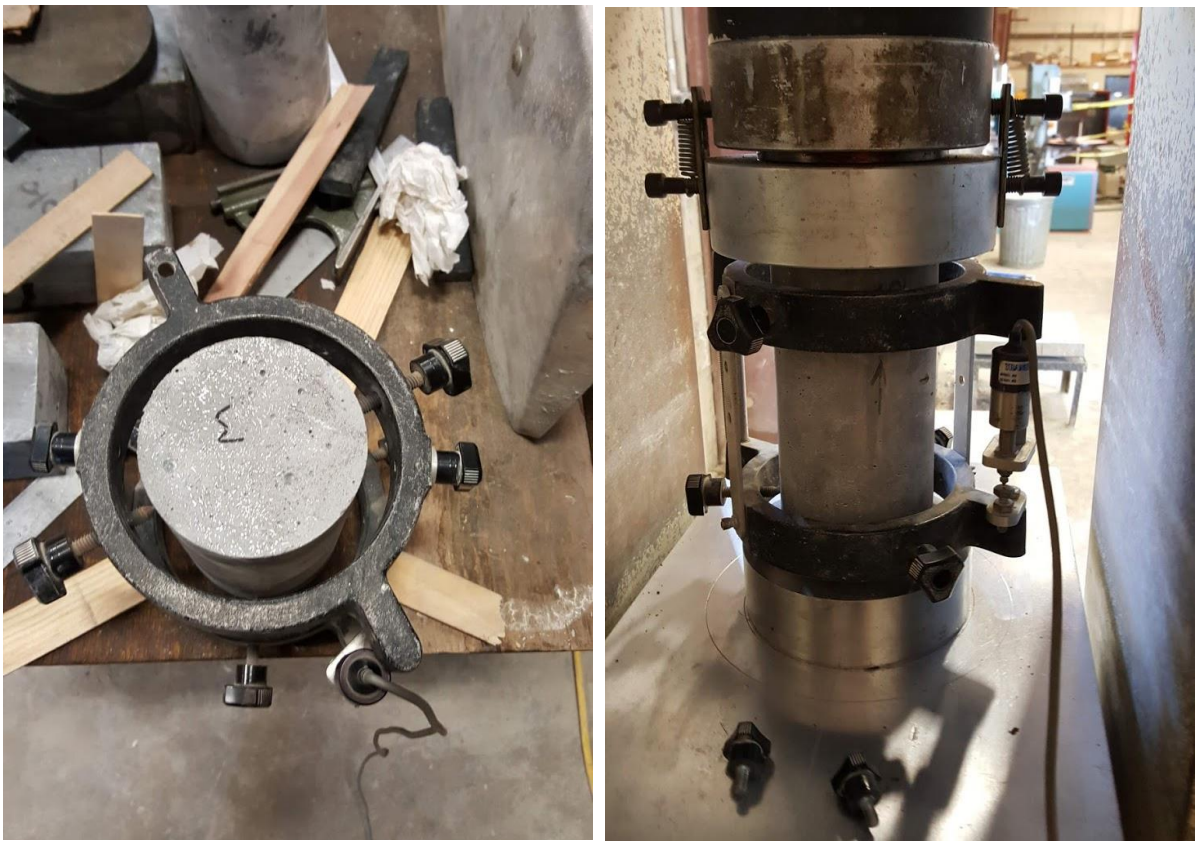

Figure 7: Standard MOE test set up

3.4.4 Splitting Tensile Strength

The splitting tensile strength testing for this research was performed on 3 in. by 6 in. cylinders. Testing was done in accordance with ASTM C496/C496M – *Standard Test Method for Splitting Tensile Strength of Cylindrical Concrete Specimens (2017)* with modification for UHPC. Prior to testing the cylinders were ground plane using a cylinder end grinder. Cylinder dimensions were then recorded using a caliper and a center line was drawn on its face to help with placing the loading plates. The specimen was then placed into the Forney machine as shown in Figure 8. The specimen was then loaded at a rate of 2.5 psi/s to failure. For the tests of specimens with 1, 2, 4, and 6% fibers, the cylinder would not fail in a typical fashion due to the fibers holding the major crack together, the test would run past what would typically be considered failure, and failure would occur due to crushing of the specimen. To determine at

what load true failure occurred the test data were downloaded from the Forney to be analyzed, but the load at break the machine showed upon completion of the test was also recorded and used as the maximum applied load. For the OU J3 mix with each fiber percentage, 3 cylinders were cast and tested at 28 days. From the data collected the splitting tensile strength was calculated using Equation 2.

$$T = 2P/\pi ld \quad (2)$$

Where T = splitting tensile strength (psi), P = maximum applied load indicated by the testing machine (lbf), l = specimen length (in.), and d = specimen diameter (in.).



Figure 8: Standard splitting tensile strength test set up

3.4.5 Flexural Strength/Modulus of Rupture

The flexural strength, also known as modulus of rupture (MOR), testing for this research was performed on 3 in. by 3 in. by 12 in. prisms. Testing was done in accordance with ASTM C78/C78M – *Standard Test Method for Flexural Strength of Concrete (Using Simple Beam w/Third-Point Loading) (2018)* with modification for UHPC. The loading rate was adjusted from 8.75 psi/s to 17.5 psi/s to account for the higher strength of UHPC specimens and the limited data storage of the machine. The loading rate was increased to this new value because the slower rate did not allow for the entirety of the test data to be recorded due to limitations of the data acquisition system. For both the OU J3 and the FIU mix with each fiber percentage 6 prisms were cast. Three were tested at 28 days and the other three at 56 days. In addition to measuring peak loads, deformation at mid-span of the specimens was measured using an LVDT to provide a measure of specimen toughness. This was done by attaching an L-bracket with fast curing glue to the side of the specimen approximately 2 cm to the right or left of the centerline or directly between the centerline and the line drawn 1.5 in. away from the centerlines. These lines were initially measured and drawn to help with the placement of the support and load plates. When the specimen was then loaded into the machine, as shown in Figure 9 (supports placed 9 in. apart), the LVDT was placed onto the edge of the L bracket and lowered until it was almost fully compressed to allow for maximum deflection measurement and then secured in place.

Upon completion of the test, the flexural strength (modulus of rupture) was calculated using the Equation 3 if the fracture that formed initiated in the middle third of the span length or using Equation 4 if the fracture occurred outside of the middle third by no more than 5% of the span length.

$$R = {}^{PL}/_{bd^2} \tag{3}$$

$$R = {}^{3Pa}/_{bd^2} \quad (4)$$

Where P = maximum applied load indicated by the testing machine (lbf), L = span length (in.), b = average width of specimen at the fracture (in.), d = average depth of specimen at the fracture (in.), and a = average distance between line of fracture and the nearest support measured on the tension surface of the beam (in.). If the fracture formed outside of either of these allowed zones, the data was discarded and replaced with a new specimen if possible.

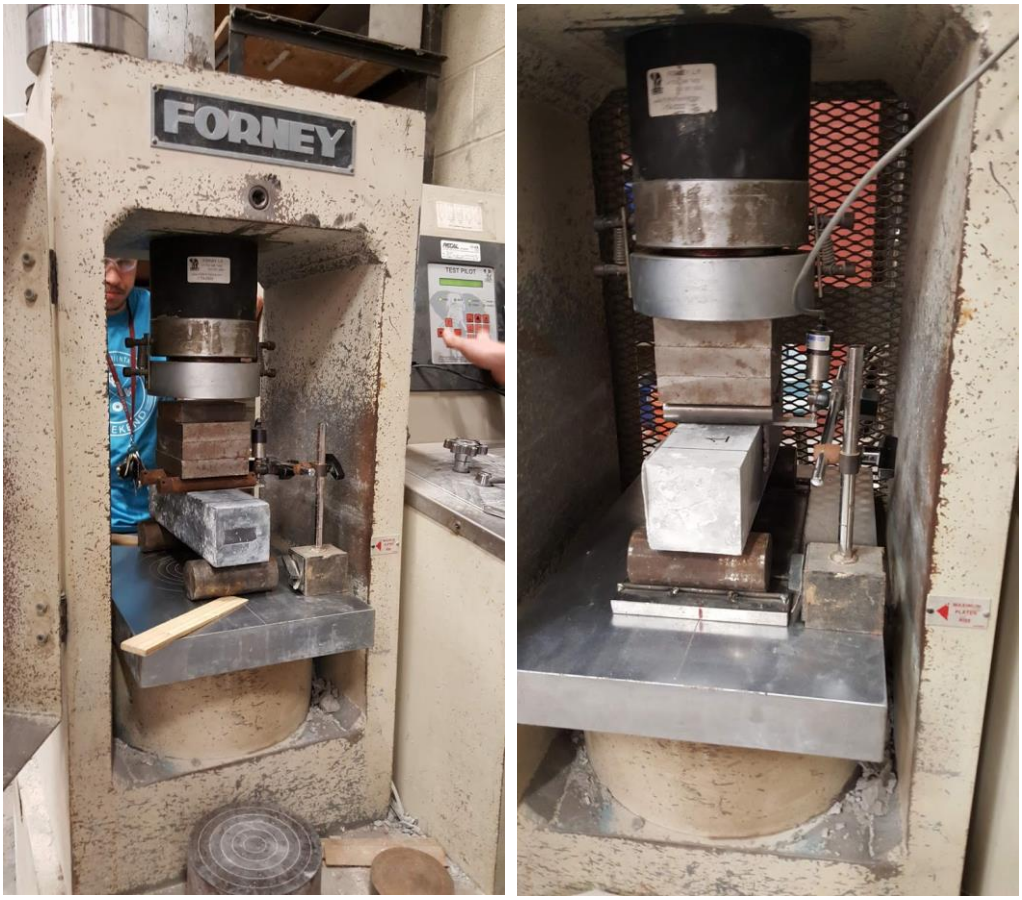

Figure 9: Standard MOR test set up

3.4.6 Freeze-Thaw

The freeze-thaw testing for this research was performed on 4 in. by 4 in. by 15 in. prisms. Testing was done in accordance with Procedure A of ASTM C666/C666M – *Resistance of Concrete to Rapid Freezing and Thawing (2019)*. Two prisms were cast and tested for each

percentage of fibers of the OU J3 mix as well as three 3 in. by 6 in. cylinders for compression testing which were tested at 28 days to compare to the other compression test results. After casting the specimens were left to cure for 14 days (3 days were spent in the molds and the rest in the curing tank) after which each all of the prisms were pulled out of the tank, dried off from excess water, and individually weighed. The specimens were dried by using a cloth to wipe off any pools of water or left out on the table to air dry for approximately 30 minutes to 1 hour prior to weighing; it was important to ensure that no excess water was dripping off them as to not add weight to the scale. It was considered acceptable if the surface itself was still saturated as long as the condition was consistent between tests since they had to remain as such to meet the required freeze-thaw test procedures. The prisms were then taken to be tested for their longitudinal resonant frequency using the James Instruments E-Meter pictured in Figure 10. The prism was centered and secured in the metal stand with an accelerometer placed at one end as can be seen in Figure 11 and then the end opposite the accelerometer was hit with a metal ball as shown in Figure 12. The resulting resonant frequency was then recorded from the E-Meter. After this test was run the prisms' height and width were measured with a caliper and then the specimens were placed in the freeze-thaw chamber as pictured in Figure 13. The machine was left to run for 36 or fewer cycles before the machine was turned off and the specimens were run through the drying and resonant frequency testing procedures as described above and in *ASTM C666.* After each of those intervals of 36 cycles or less was complete the prisms had to be thawed out from the last freeze cycle. This was most often done by leaving them in the freeze chamber overnight or for several hours during the day with it turned off and the lid was often left open if faster thawing was required. After the specimens had thawed enough to remove them from the freeze chamber, they were placed back in the curing tank if testing them immediately was not plausible. These

procedures were repeated every cycle interval. The total number of cycles for the test was adjusted from the 300 specified in ASTM C666 to 350 to examine the possibility of deterioration after the normal test duration due to the higher strength and known high durability of UHPC.



Figure 10: James Instruments E-Meter device used to record resonant frequency data during the freeze-thaw test



Figure 11: Freeze-thaw test specimen set up set up to measure resonant frequency

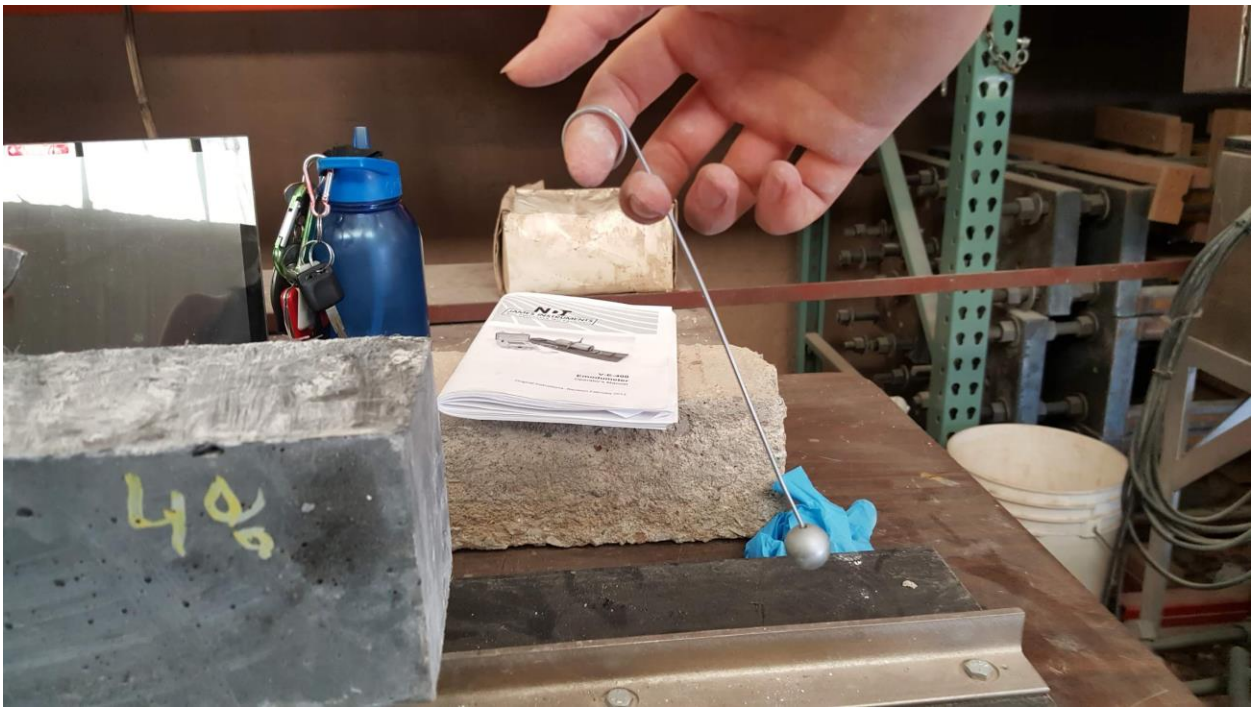

Figure 12: Metal ball and distance of hit used to determine resonant frequency for the freeze-thaw tests



Figure 13: Freeze-thaw specimens in the freeze-thaw chamber

Chapter 4: Results and Discussion

4.1 University of Oklahoma J3 Mix

4.1.1 Flowability

Table 3 shows the measured flow values and HRWR contents for each of the OU J3 mixes. The data show a decrease in flow with increase in fiber content and increase in required HRWR at 4 and 6% fibers. For one of the 4% trial mixes the same 18 oz/cwt of HRWR was used and no or minimal flow was detected. The mixture was stiff due to the quantity of the fibers and impossible to work with.

Table 3: OU J3 flow test results

Percent Fibers (%)	Flow (in.)	HRWR (oz/cwt)
0	9.5	18
1	9.5	18
2	9.5	18
4	8.25	23
6	4.5	28

The flow remained consistent for 0, 1, and 2% steel fibers and a constant HRWR with all three overflowing off the side of the flow table as can be seen in Figures 14-16. As the fiber content increased the mixture became more stiff and the fibers formed a clump in the center of the flow which can be seen in Figures 17 and 18. The HRWR was increased for the 4 and 6% fiber mixes to achieve adequate workability. The final flow test for the 6% fiber mixture consisted of two measurements. One was the diameter of the clump of fibers in the center that was measured at 4.5 in., the other was of the more flowable concrete spreading beyond the main cluster which was measured at 5 in., the visual representation of this can be found in Figure 18

which was captured right after the measurements were taken. The smaller measurement was reported since that was where the majority of the concrete mixture settled. As a result of the decrease in flow, the concrete mixture for 4 and 6% fibers was more difficult to work with and the mixtures lost workability and became unusable more quickly. This was most evident in the 6% fiber mixture as it was very dense with steel fibers as can be seen in Figure 19, which shows the 6% batch right after mixing. The most significant issue with the higher percentages of fibers was segregation of the fibers from the rest of the concrete mixture. This segregation resulted from the increase in HRWR, but without increasing the HRWR content the mixture would have been impossible to work with. It must also be noted that segregation was not an issue until the 6% fiber mix pour whereupon removing the concrete from the mixer it was noticeable that many fibers settled at the bottom of the container that was used to transport the concrete to the forms. So, it is possible that the fibers were unevenly distributed in the concrete placed in the specimen forms and the final tested specimens had less than six percent fibers by volume on average. This may have also affected the results of other tests such as the compression or MOR tests where a higher fiber content resulted in failure at a higher load. If said segregation occurred, then some specimens may have ended up consisting of a smaller percent fibers by volume than intended and thus lower stress at failure.



Figure 14: OU J3 0% fiber mix flow test



Figure 15: OU J3 1% fiber mix flow test



Figure 16: OU J3 2% fiber mix flow test



Figure 17: OU J3 4% fiber mix flow test



Figure 18: OU J3 6% fiber mix flow test



Figure 19: OU J3 6% mixture immediately after mixing

4.1.2 Compressive Strength

The results for the cylinder and cube compression tests are displayed in Tables 4 and 5 and in Figures 20 and 21, respectively. Each value is an average of three trials, but data for the individual specimens tested for each percentage of fibers can be found in Table 17 in Appendix C, which shows the range of values for the individual tests. As can be seen in both Figure 20 and Figure 21, in general the compressive strength increased with increasing percentage of fibers in the specimens. The compressive strength also increased with time and while the specimens gained more than half of the final strength by day 3 as typical with most concrete, the specimens gained the rest of the 56-day strength over the next 53 days. For the cylinder specimens (Figure 20) there is a drastic deviation in the trend for the 1% fiber mix at 28 days. The source of this deviation is uncertain though the results for each of the three trials was as follows – 13051, 11176, and 15521 psi. This is a wider spread of results than was typical; for other percentages the greatest difference between individual cylinders for 28 days did not exceed 2,128 psi such as in the case of the 2% fiber mix, while in this case for 1% fiber mix the difference is 4,345 psi between two of the results. It must also be noted that on average and all three individually, the 1% fiber mix results are smaller than the 0% fiber mix results for 28 days.

Table 4: OU J3 cylinder compressive strength test data for each steel fiber content

Concrete Age (days)	**0%**	**1%**	**2%**	**4%**	**6%**
3	12,590	12,170	12,540	11,850	12,460
7	13,240	13,410	14,480	14,500	14,820
28	16,380	13,250	17,220	17,490	17,510
56	16,940	17,020	18,150	17,620	18,320

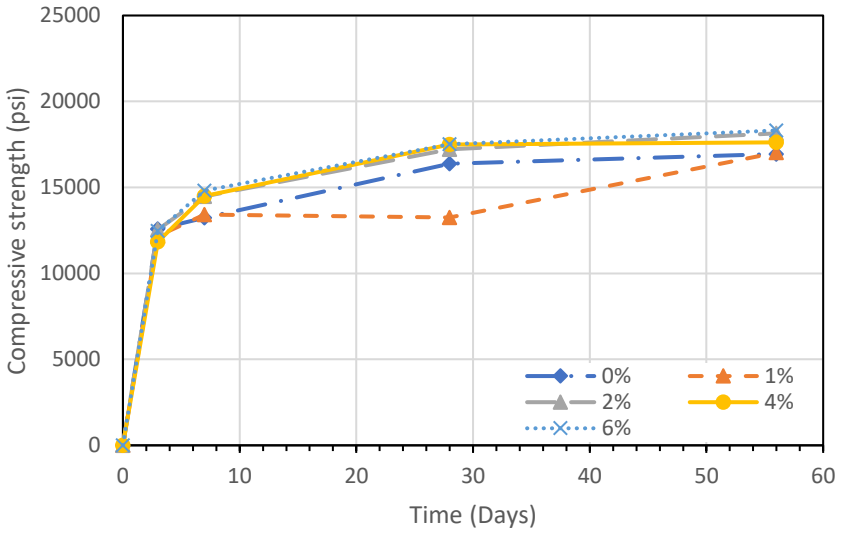

Figure 20: OU J3 cylinder compressive strength test results

Contributing factors could have been air pockets within the specimens which could have resulted from poor consolidation and were unable to escape due to the quickly deteriorating flowability once the HRWR wears off, or it is possible that uneven distribution of fibers within the cylinders could have been the cause. Another possible explanation is inconsistency in testing procedure for this specific set of three cylinders since the cylinders performed as expected for all other testing days. This could have occurred at any point in the process, but the most likely culprit is either the grinding of the specimens, which could have been insufficient and instead exposed a weak point in the specimens such as an air pocket, or the setup of the testing mechanism. The fact that this test data point is a deviation can also be confirmed by looking at the cube results and the graph in Figure 21 where the compressive strength for the 1% fiber mix at 28 days increased in accordance with the overall trend. Based on further analysis of the data from both the cylinders and the cubes, it can also be noted that the compressive strength of the 2 and 4% fiber mixes are very close to each other, almost identical. The outlier of the 1% fibers results makes it harder to see in Figure 20, but Figure 21 shows it very clearly. This suggests that

with a larger amount of steel fibers, the increase in strength is almost negligible between 2 and 4%. While the fibers increased by 264.5 lb/yd^3 or 100% in this batch of this mix design, the strength only increased by 270 psi or just 1.5% if looking just at the 28 days data for the cube 2 and 4% specimens. The increase is only 60 psi or 0.3% for the 56 day testing window for these specimens. It should also be noted that for the cylinder specimens the 2% fiber mix tested at 56 days had a higher compressive strength than the 4% fiber mix and for the cube specimens the compressive strengths were approximately the same. Besides these two deviations, it appears that the rest of the data is fairly consistent and expected with compressive strength increasing with increase in fiber percentage. The strength of the concrete increased rapidly to the 3-day testing window and continued to increase but at a progressively slower rate for each of the following testing windows (7, 28, and 56 days).

Table 5: OU J3 cube compressive strength test data for each steel fiber content

Concrete Age (days)	**0%**	**1%**	**2%**	**4%**	**6%**
3	11,660	11,320	12,090	12,530	14,210
28	14,430	15,730	18,170	18,440	19,670
56	15,270	17,470	18,630	18,690	21,610

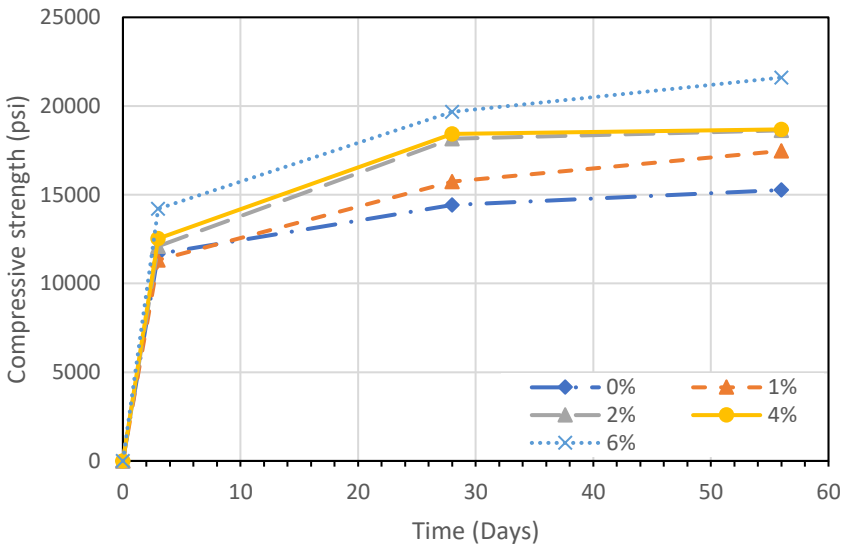

Figure 21: OU J3 cube compressive strength test results

Besides the numerical data, the physical evidence was just as telling. As might have been expected the 0% fiber specimens experienced sudden failure and after undergoing failure they crumbled into pieces as can be seen in Figures 22-26. Meanwhile with any amount of fibers present in the specimens, even after failure the concrete stayed together and minimal flaking occurred as can be seen in Figures 27-42. Figures 22-42 are representative of the discussion, but additional pictures that show the result of each individual compression test can be found in Appendix A in Figures 116-124. Compressive strength increased with increased steel fiber percentages as well as increased curing time. This was most evident in the data. Besides the 0% as compared to the other percentages, the specimen failures for the other fiber contents did not show the change in strength as clearly, though small changes in the way that specimens failed as compared to each other within the same batch can be noted. The 0% specimens for all days of testing crumbled into pieces, but there was a progression in how much these specimens stayed together as the concrete aged and gained strength. The cylinder remained slightly more intact for day 3 testing as they stayed together when picked up and transferred from the Forney onto a

table, but completely disintegrated into pieces upon the 56 day testing and were impossible to transfer over in one piece. This transition can be clearly seen in Figures 22-25. This can be attributed to the concrete getting harder with age as it cured and therefore becoming more brittle, but also stronger. Meanwhile, as the fiber percentage increased, it appears that more flaking along the lines of failure began to appear. This was first observed in the 2% fiber 56 day cylinders as can be seen in Figure 30 and also noted in the 2% fiber 56 day cube specimens but to a smaller extent as can be seen in Figure 32. In comparison, the 2% fiber 28 day specimens (cylinders Figure 29 and cubes Figure 31), while still experiencing cracking at a high load, did not experience flaking to nearly the same extent. This is most likely due to the same reasons as discussed for 0% as well as the fibers playing an additional role in holding these more brittle pieces of concrete in place, allowing the specimen to undergo additional deformation before the specimen failed under load. This trend continued as more flaking began to occur with increasing percentage of fibers as well as longer curing time as can be seen for 4% (Figures 33-36) and 6% fibers (Figures 37-42), though the 6% had an outlier. The middle specimen depicted in Figure 37, which corresponds to the 6% 3 day batch, compressed much further than any of the other compression specimens tested for J3 and experienced more flaking when tested in the same way as the others. It is uncertain why this occurred as the setting for the loading rate and when to stop the test remained the same for that set of specimens. The 6% fiber 3 day cubes (Figure 40) also appear to have more flaking than their counterparts at 28 or 56 days (Figures 41 and 42).

Besides these differences, the failure type that the specimens experienced remained consistent. Between the different testing days of the same percentage or between or same days of different percentages, there appears to be no visual difference (besides what was discussed previously) between the specimen failures. It is challenging to identify what kind of failure the

specimens underwent due to many cracks forming along the surface before total failure could occur because of the steel fibers holding the initial failure together, but it appears that the cylinder specimens developed a Type 1 fracture pattern (ASTM C39) based on the evidence from the 0% fiber specimens as can be seen in Figures 22-25, while with higher percentage of fibers the patterns began to resemble Type 2 and 3 fractures.



Figure 22: OU J3 0% cylinder 3 day compressive strength test specimens after failure



Figure 23: OU J3 0% cylinder 7 day compressive strength test specimens after failure



Figure 24: OU J3 0% cylinder 28 day compressive strength test specimens after failure



Figure 25: OU J3 0% cylinder 56 day compressive strength test specimens after failure



Figure 26: OU J3 0% cube 28 day compressive strength test specimens after failure



Figure 27: OU J3 1% cylinder 28 day compressive strength test specimens after failure



Figure 28: OU J3 1% cube 56 day compressive strength test specimens after failure



Figure 29: OU J3 2% cylinder 28 day compressive strength test specimens after failure



Figure 30: OU J3 2% cylinder 56 day compressive strength test specimens after failure



Figure 31: OU J3 2% cube 28 day compressive strength test specimens after failure



Figure 32: OU J3 2% cube 56 day compressive strength test specimens after failure



Figure 33: OU J3 4% cylinder 28 day compressive strength test specimens after failure



Figure 34: OU J3 4% cylinder 56 day compressive strength test specimens after failure



Figure 35: OU J3 4% cube 28 day compressive strength test specimens after failure



Figure 36: OU J3 4% cube 56 day compressive strength test specimens after failure



Figure 37: OU J3 6% cylinder 3 day compressive strength test specimens after failure



Figure 38: OU J3 6% cylinder 28 day compressive strength test specimens after failure



Figure 39: OU J3 6% cylinder 56 day compressive strength test specimens after failure



Figure 40: OU J3 6% cube 3 day compressive strength test specimens after failure



Figure 41: OU J3 6% cube 28 day compressive strength test specimens after failure



Figure 42: OU J3 6% cube 56 day compressive strength test specimens after failure

4.1.3 Modulus of Elasticity

For each individual steel fiber percentage, a new maximum load was calculated for the specimens. This calculation was based on 40% of the measured compressive strength and the specimen diameter and can be found in Table 6 alongside the calculated chord modulus of elasticity (MOE) and whether this data was based on the cylinder or the cube compressive strength data. Presented MOE data are averages of three specimens and two tests per specimen.

Table 6: OU J3 modulus of elasticity data

Percent Fibers (%)	**Compression Data Specimen Type**	**Load (lb)**	**Chord Modulus of Elasticity (psi)**
0	cylinders	82,328	5,280,000
1	cubes	79,089	5,420,000
2	cylinders	86,550	5,650,000
4	cylinders	87,914	5,640,000
6	cylinders	87,998	6,030,000

The low compressive strength of the 1% cylinders at 28 days mentioned in section 4.1.2 would have changed the load value used in the modulus of elasticity (MOE) test. However, to prevent such a large deviation, the cube results were used instead. The compressive strength of the cubes was higher than that of the 1% cylinders and was in line with the increasing strength trend when compared to the cube results for the rest of the fiber percentages, but it was still lower than the compressive strength of the rest of the cylinders and therefore could have a limited impact on the data. As can be seen in Figure 43, the results for the 1% fiber specimens appear to be consistent with the trend seen in the graph and it is the 4% data that breaks the increasing trend. However, the 4% fiber mix has a result very similar to the 2% fiber specimens, which follows the trend seen for compressive strength. The individual specimen results for 4% fiber mix were as follows – 5,431,000 psi, 5,646,000 psi, 5,850,000 psi. Based on this spread it appears that only one of the specimens out of the three was greater than the average of the 2% specimens. It is possible that, similarly to the discussion on compressive strength, this again was due to air pockets, or fiber settlement, or inconsistent grinding, or even poor placement in the compressometer. More testing is required to determine if the 4% fiber mix and 2% fiber mix have similar properties or if the results were gotten in error. By looking at the data overall it can be seen that indeed the modulus of elasticity of UHPC, or more specifically of J3, is in the higher range for MOE of conventional concrete, which typically ranges from 2,000,000-6,000,000 psi. Higher MOE represents a stiffer specimen, while lower MOE represents a specimen that deforms more easily. This corresponds to the results seen in Figure 43, the 6% fiber specimens has the highest MOE as the steel fibers give it greater strength but also greater stiffness. Thus, it is possible that this phenomenon could be just be a function of replacing a volume of the concrete with steel, which has a higher modulus of elasticity.

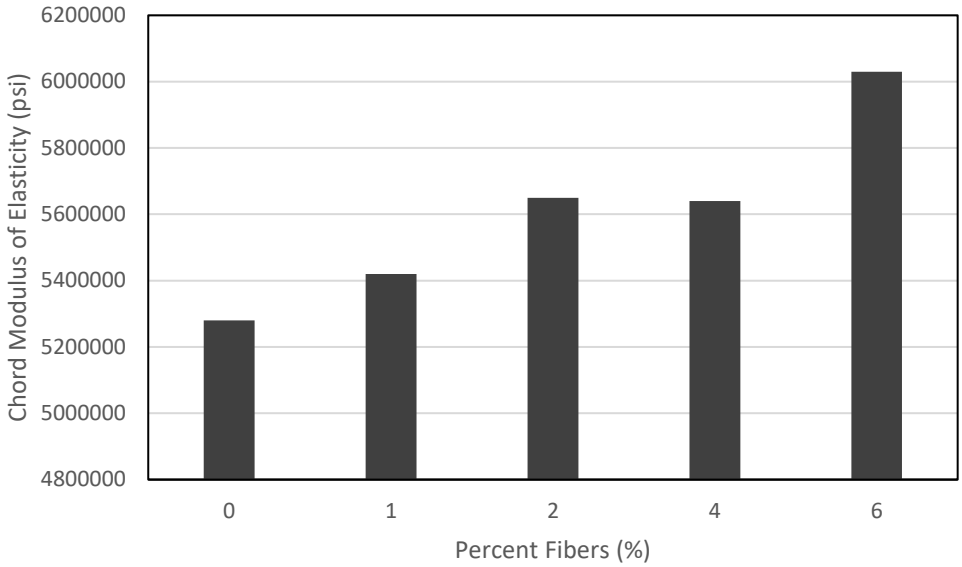

Figure 43: OU J3 MOE results

4.1.4 Splitting Tensile Strength

The averages of the data gathered from the splitting tensile strength test are given in Table 7 and Figure 44. Each average is a result of 3 specimens; data for the individual specimens tested for each percentage of fibers can be found in Table 18 in Appendix C. In general, the splitting tensile strength increases significantly with increasing steel fiber content. However, the 6% fiber specimens had a lower splitting tensile strength than the 4% fiber specimens. The difference is not drastic, only a 159 psi (or approximately 5%) decrease, but it is uncertain what could have caused this deviation from the trend. Based on the recorded dimensions of each specimen, the average of the 6% cylinders had a higher height than that of 4%. It is also true that greater height would have resulted in a lower splitting tensile strength based on the equation used to calculate it, though the difference between the 4 and 6% cylinder height is only approximately 0.3 inches. It is possible that this difference in dimensions accounts for some deviation in the test results, though there are other factors that must be considered. During the test, especially for the higher percentage specimens, the cylinder would begin developing flat spots on top and bottom

from the loading plates crushing it during testing. This would begin to happen most often after the maximum load had been reached, but the test would not end yet since the machine was set to run until the strength of the specimen would fall below 50% of this maximum load. It is a concern that this might have affected the data for the 6% fiber specimens as an incorrect load (compressive vs tensile) may have been recorded by the machine, though it is also possible that splitting tensile strength just did not benefit from the additional steel fibers beyond 4%.

Table 7: OU J3 splitting tensile strength test results

Percent Fibers (%)	Load at Break (lb)	Splitting Tensile Strength (psi)
0	29,030	1,030
1	53,485	1,995
2	71,420	2,580
4	82,250	3,085
6	83,120	2,925

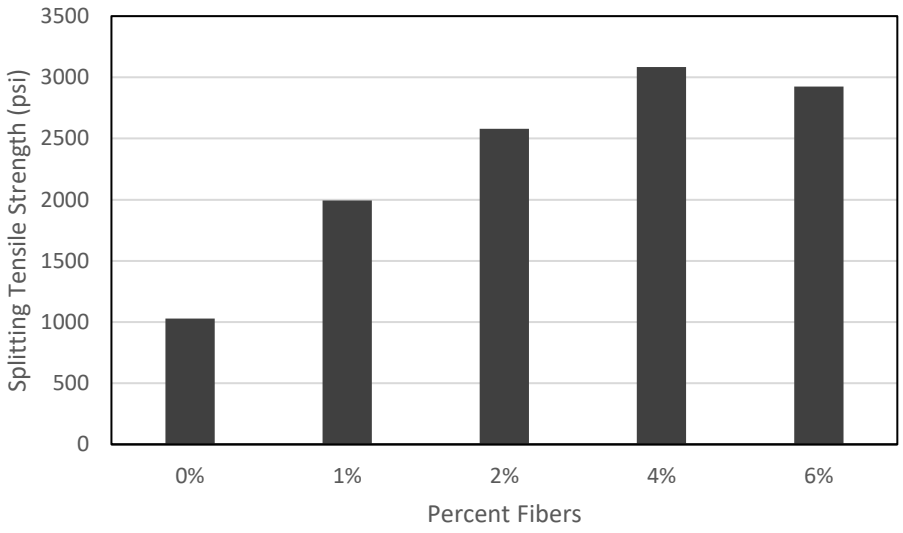

Figure 44: OU J3 split cylinder test

Visually the results were similar to the cylinder compressive strength tests with the 0% undergoing a sudden failure into two major pieces that separated relatively cleanly as shown in Figure 45, while the 1, 2, 4, and 6% fiber specimens (Figures 46-49) only experienced cracking

and flaking even upon failure, which was defined to be when the specimens could no longer hold 50% of the maximum load. Most of the 0% fiber specimens formed a crack right down the middle as can be seen in Figure 45 and failed along that crack as is typical for this type of test. However, for the rest of the specimens, the fibers held the specimen together and did not allow the typical failure to occur. Most of the time in this case, the specimen would form several cracks on the surface in the middle region or develop a more prominent crack off center surrounded by smaller cracks. As the percentage of fibers increased to 4 and 6%, the cracks that formed became more irregular in direction and sporadic in pattern (Figures 48 and 49). This is possibly due to the fracture following the path of least resistance within the matrix and the excess amounts of steel fibers preventing typical splitting behavior. It must be noted that besides fibers, there is no other component in the mix that would affect cracking behavior. The concrete itself is uniform as there are no aggregate particles larger than sand, thus the difference in performance would be due to fiber distribution and how the fibers are oriented.



Figure 45: OU J3 0% 28 day splitting tensile test specimens after failure



Figure 46: OU J3 1% 28 day splitting tensile test specimens after failure



Figure 47: OU J3 2% 28 day splitting tensile test specimens after failure



Figure 48: OU J3 4% 28 day splitting tensile test specimens after failure



Figure 49: OU J3 6% 28 day splitting tensile test specimens after failure

4.1.5 Flexural Strength/Modulus of Rupture

The modulus of rupture (MOR) was a challenging test to conduct as there were many potential sources of error and variation due to the small specimen size and required precision for placement of the testing set up. However, most of the specimens cracked in the intended middle third region. The results for 28 and 56 day testing can be seen in Table 8 and Figure 50, which were based on maximum load the specimens experienced. These results are an average of three specimen for each fiber percentage. Based on this data, it is clear that with increase in time the concrete had to cure, the strength also increased. In general, the strength increased with increase of percent of fibers, but the 6% fiber mix did not follow this trend at 28 or 56 days. This could be due to operator or machine error as described below or due to reduction of strength as the number of steel fibers is increased beyond a certain point where their magnitude takes away from the strength that the concrete itself contributes. Fiber segregation was also an issue with the 6% mix (and less so with the 4%) since fibers would have settled at the bottom of the specimen and the prism had to be rotated to conduct the test such as that the top and bottom were then the sides. Because of this rotation to the side, the new tension face was not the one with the highest concentration of fibers to properly test the effect of 6% fibers by volume.

Table 8: OU J3 flexural strength (MOR) for each steel fiber content

Concrete Age (days)	**0%**	**1%**	**2%**	**4%**	**6%**
28	1,265	1,765	2,450	4,280	3,560
56	1,735	2,470	3,040	4,140	4,140

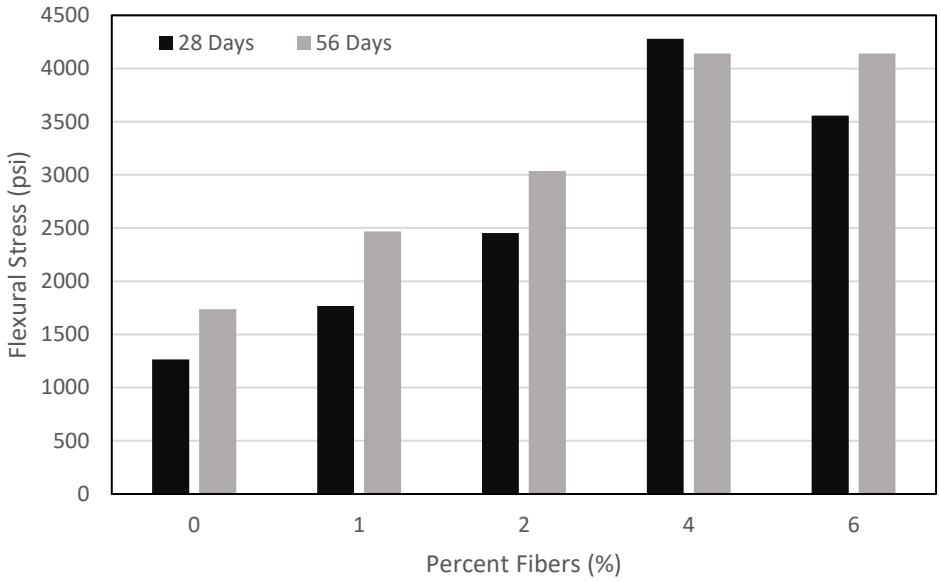

Figure 50: OU J3 MOR maximum load at 28 and 56 days

Though alternatively, looking carefully at the data in Figure 50 once more, it could be that the 4% fiber batch had a higher strength than expected based on this test and the splitting tensile strength results discussed earlier. It appears that in both tension tests (splitting tensile, MOR) the 4% is the outlier. Looking at Figure 50, it appears that the increase in flexural stress follows an upward trend and if the 4% fiber data was not present in the graph, then the 6% fiber data would match that trend and the curve it forms. Additionally, the 4% fiber results are the only ones where 28 day strength exceeds 56 day strength and its 56 day strength is practically the same as the 6% fiber 56 day strength. The individual test results for the 4% mix at 28 days were as follows – 3,750 psi, 5,168 psi, 3,924 psi. For this set of tests nothing was out of the ordinary in terms of setup and loading (no preload higher than 1,500 lb) to account for the slightly higher strength specimen. The individual test results for the 4% fiber mix at 56 days were as follows – 4,600 psi, 3,526 psi, 4,299 psi. A total of five specimens were tested, but the third out of five had to be discarded because the machine failed to record the test data and the first out of five did not meet the fracture within the proper length of specimen requirement. During testing, the first three

specimens were not placed properly within the machine; the loading plates were slightly off center and could have caused the specimens to break outside the middle third as well as at a greater load indicating a higher strength. It is also for this reason that two additional specimens were tested, but it must be noted that they were cast as shrinkage specimens and were 1 in. shorter as discussed further below.

In addition to factors that could have artificially increased the MOR results for the 4% fiber specimens, some other factors came into play with the 6% specimens that could have potentially lowered the overall results for this batch. During the 28 day testing four specimens were tested and the results were calculated as follows – 4,113 psi, 4,680 psi, 2,574 psi, 2,864 psi. The fourth specimen was tested due to the significant change in strength between the first two specimens to the third. A confirmation was required whether the results of the third specimen were an outlier. The fourth specimen closely matched the results of the third providing an even split of the results. This could have been due to the aforementioned segregation and settlement of fibers for the 6% mix, though in this case some excessive preloads may have played a role as well. The third specimen was unintentionally preloaded to almost 3,000 lb (the preload should not have exceeded 1,500 lb as that is when the machine starts recording the data for the LVDT gauge). This could have had an effect on the strength by overstressing the specimen too fast causing it to fail at a lower load. Additionally, the fourth specimen was unintentionally left to load at a rate of 167 psi/s as the loading rate on the machine was difficult to regulate, as was the preload. It was left at this rate for less than a minute, but this too could have affected the results. For 56 day testing these issues were not encountered and the following were the results for each of the three 6% fiber specimens – 4,058 psi, 3,756 psi, 4,608 psi. Data for the individual specimens tested for each percentage of fibers can be found in Table 19 in Appendix C, which

shows the range of values for the individual tests.

To further help determine the trend of this data and help isolate the effects of compressive strength, the tensile strength values were normalized by the square root of the cylinder compressive strength to help separate out those variations and isolate the effect of the fibers (Figure 51). This prediction of the flexural stress multiplier is not perfect because of the effect of steel fibers on compressive strength, but the normalized strength definitely increases with increase in fiber content and each of the multipliers is greater than that of 7.5 used for traditional concrete.

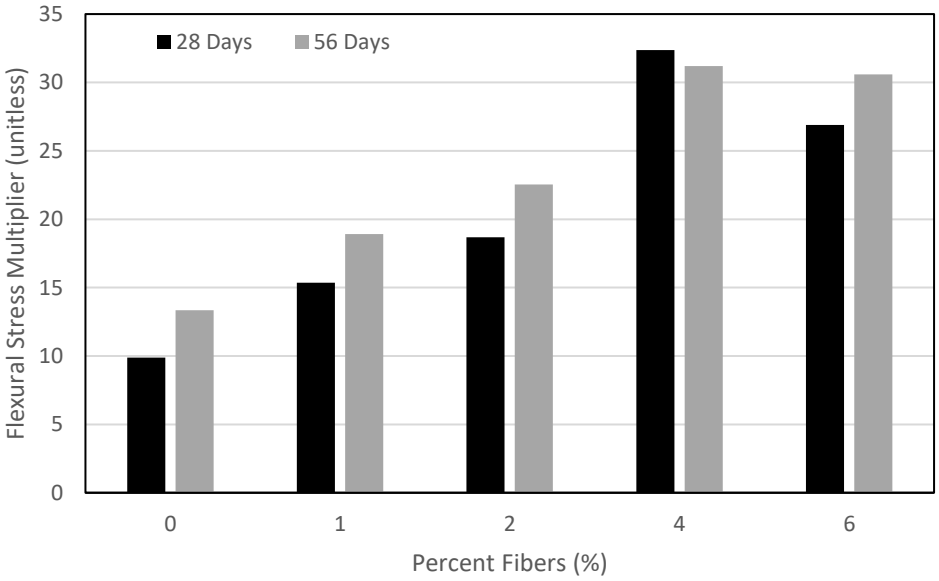

Figure 51: OU J3 MOR results normalized by square root of compressive strength

Overall, other than for the 4% fiber mix, the data show that the modulus of rupture was consistently higher for 56 day testing window than for 28 days though there was not a consistent magnitude difference between the two values. For the 0% mix the difference was 470 psi or 37%, for the 1% mix 701 psi or 40%, for the 2% mix 585 psi or 24%, and for the 6% mix 583 psi or 16%. This averaged out to 29% increase between the 28 and 56 day specimens. It appears that the difference decreased with increasing fiber content which could indicate that the fibers were

more of a controlling factor for higher percent fiber mix than for the lower fiber percentages. Most of the specimens cracked in the intended middle third region of the span length as can be seen in Figures 52-61. However, for 28 day testing, the first specimen of the 2% fiber mix, the second of the 4% fiber mix, and the fourth of the 6% fiber mix cracked in the tension surface outside of the middle third of the span length as can be seen in Figures 54, 55, and 56. A proper equation from ASTM C78 was used to account for this in the case of these specimen as well as for any other specimens that fractured outside of the middle third of the span length. As can be seen in Figure 60 this also occurred with the second (first specimen in picture) and fifth (third specimen in picture) of the 4% fiber specimens at 56 day testing (in Figure 60 only 3 specimens are shown because first and third were discarded for reasons mentioned previously in this section). It is uncertain if these specimens cracked outside of the desired region due to that being the greatest point of weakness within the specimen or because of poor placement of the specimen under loading. It was challenging to get the prisms perfectly centered in the compression machine. The small dimensions of the specimens left little margin for error, and while it did not appear to necessarily affect the maximum load that the specimen reached, it did affect crack location. Even minor misalignment would cause the fracture to develop on the edge of the middle third while very few specimens fractured closer the middle. Setting a consistent loading rate was challenging for this particular compression machine as well, which meant that some specimens were loaded to the failure load faster than others which may have affected the results. Due to these different sources of uncertainty, four or five specimens were tested for some of the percent fiber mixes instead of just three. For these cases where extra specimens were needed there typically was no extra 3 in. by 3 in. by 12 in. specimen left over so an extra 3 in. by 3 in. by 11 in. ASTM C147 shrinkage specimen had to be used. While this prism was 1 in. shorter, the

cross-section was the same and the supports could still be placed the same distance apart as with the specimens constructed for the modulus of rupture test. The specimens whose data was deemed unusable are not shown in the figures nor were they include in the data analysis.

As evident from the data in Figure 50 as well as from the visual evidence in Figures 52-61, the fibers made a tremendous difference in the performance of the specimens. At 0% fibers the specimens experienced brittle sudden failure and separated into two pieces, while with any additional amount of fibers the two halves stayed together, the crack formed slowly, and the specimen deflected and slowly separated at the crack over time until more and more of the fibers became exposed. In some instances, some of the many fibers pulled out of the concrete as the crack widened and some of the fibers may have fractured from the tension. In many cases the failure crack was diagonal or had some deviation from purely vertical, as can be seen in two out of the three specimens in Figure 57, and less often it was purely vertical, as is typically seen for concrete modulus of rupture. In fact, some of the 0% specimens had what appeared to be a curved diagonal crack (Figure 57). With increased percentage of fiber reinforcement, the failure crack tended to deviate more from purely vertical and became more of an irregular wave pattern likely following weak points in the concrete as seen in Figures 55, 56, 60, and 61. These irregular diagonal cracks could indicate failure due to shear instead of flexure within the specimens. As the percentage of fibers increased, the amount of exposed fibers that could be seen through the developing crack also increased. Looking at these cracks it can also be noted that the orientation of the fibers within the specimen would have played a major role in its strength as the more fibers were in a horizontal position (perpendicular to the forming crack) the stronger the specimen would be. The distribution and concentration of the fibers throughout the specimen would have also played a major role especially noting the discussion of the segregation

of fibers within the 4 and 6% fiber mixes. If the fibers did settle at the bottom of the specimen while curing then the fiber distribution was not uniform across the specimen and the specimen was not in the optimal position for highest strength during testing as it had to be turned to its side to ensure flat sides on the top and bottom for load and support placement.



Figure 52: OU J3 0% 28 day MOR test specimens after failure



Figure 53: OU J3 1% 28 day MOR test specimens after failure



Figure 54: OU J3 2% 28 day MOR test specimens after failure



Figure 55: OU J3 4% 28 day MOR test specimens after failure



Figure 56: OU J3 6% 28 day MOR test specimens after failure



Figure 57: OU J3 0% 56 day MOR test specimens after failure



Figure 58: OU J3 1% 56 day MOR test specimens after failure



Figure 59: OU J3 2% 56 day MOR test specimens after failure



Figure 60: OU J3 4% 56 day MOR test specimens after failure



Figure 61: OU J3 6% 56 day MOR test specimens after failure

4.1.6 Freeze-Thaw Mix

It must be noted that the mix used for all of the freeze-thaw related tests discussed under section 4.1.6 is still the OU J3 mix, but these specimens will be referred to as the freeze-thaw specimens for ease of clarification as they were cast from different batches and included their own set of flowability tests and compressive strength cylinders. These will only be referred to as the OU J3 specimens in section 4.1.6.3 as that discusses the freeze-thaw test itself.

4.1.6.1 Flowability

A flow test was run every time a new batch was mixed which included the five batches mixed to cast the freeze-thaw specimens. These flow test results, shown in Table 9, closely matched the initial OU J3 flow test results. In this set of tests the 0 and 1% fiber mixes overflowed off the side of the table, while the 2% fiber mix only flowed to one edge of the flow table and the 4 and 6% fiber mixes had a slightly larger flow compared to the initial OU J3 tests. The latter was most likely due to the shorter time required to mix a smaller volume batch for these pours so the HRWR was still acting at its full strength. The 6% fiber flow test for the freeze-thaw specimens is shown in the right image of Figure 62 as it had the most noticeable change in flow compared to the earlier J3 batch shown in Figure 18. The left side of Figure 62 shows the 6% J3 flow once again for direct comparison to the freeze-thaw results.

Table 9: Freeze-thaw flow test results

Percent Fibers (%)	**Flow (in)**	**HRWR (oz/cwt)**
0	9.5	18
1	9.5	18
2	9	18
4	8.5	23
6	5.25	28



Figure 62:OU J3 (left) vs. freeze-thaw J3 (right) 6% fiber mix flow test

4.1.6.2 Compressive Strength

It must be noted that a different Forney machine was used to collect the compressive strength data for the freeze-thaw specimens. This should not be an issue because both machines were calibrated accurately and the same procedures were used with each machine to ensure accurate results. The greatest difference was the more manual operational requirements for the Forney used for this set of tests. A comparison of the compressive strength data between the 28 day test results from the initial J3 batches and those mixed for the freeze-thaw specimens are shown in Table 12 and Figure 63.

Table 10: Freeze-thaw vs. OU J3 28 day cylinder compressive strength test results for each steel fiber content

Mix Type	**0%**	**1%**	**2%**	**4%**	**6%**
Freeze-Thaw	12,440	12,890	13,700	15,010	16,630
OU J3	16,380	13,250	17,220	17,490	17,510

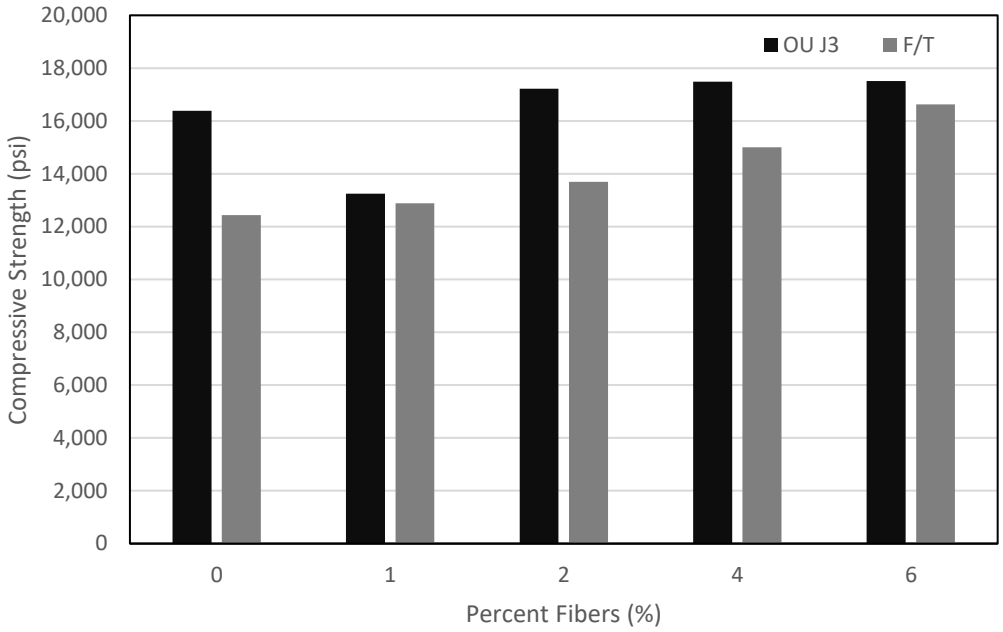

Figure 63: Freeze-thaw vs. OU J3 28 day cylinder compressive strength test results

The freeze-thaw batches have a more gradual and consistent increase in strength as the percent of fibers increases compared to the initial J3 compression tests, which show an almost negligible increase in compressive strength between the 2, 4, and 6% fiber mixes. Based on Figure 63, the two that most closely match are the results for the 1% fiber mixes, which was shown to be an outlier at 28 days in the previous J3 compression tests with a smaller value than expected. It is unclear as to why the J3 28 day compressive strength tests and the 28 day freeze-thaw batch compressive strength results do not match more closely, but it is possible to attribute this to inconsistencies within concrete for it is often an imprecise medium. All of the mixing and testing procedures were followed precisely for both mixes. The only differences were that a new bucket of HRWR was used for the freeze-thaw specimens and the cylinders were possibly ground down more to remove air bubbles on the surface. The Forney machine was still set to 6 in. tall specimens, and the smaller specimen height would have resulted in higher strength. It is also possible but unlikely that using a different Forney machine could have caused the observed

deviation between the results. There is no visual evidence of what could have caused this deviation as the failure the specimens underwent, which can be seen in Figures 64-68, closely matched the compression failures described previously in the OU J3 section in pattern and type. Just like with the failure behavior observed for the OU J3 specimens, the freeze-thaw cylinders also experienced increased flaking with increased percentage of fibers, which indicates that they experienced higher load and the fibers held the pieces that were beginning to fall off together thus allowing for the specimen to take on that higher load. The cracks that develop for the 1% cylinders (Figure 65) appear almost vertical, but as the volume of fibers reaches 6% (Figure 68) the cracks appear more irregular and aggressive, once again similar to what was seen with the OU J3 specimens.



Figure 64: Freeze-thaw 0% 28 day cylinder compressive strength test specimens after failure



Figure 65: Freeze-thaw 1% 28 day cylinder compressive strength test specimens after failure



Figure 66: Freeze-thaw 2% 28 day cylinder compressive strength test specimens after failure



Figure 67: Freeze-thaw 4% 28 day cylinder compressive strength test specimens after failure



Figure 68: Freeze-thaw 6% 28 day cylinder compressive strength test specimens after failure

4.1.6.2 Freeze-Thaw

The freeze-thaw test was conducted on two 4 in. by 4 in. by 15 in. prisms for each percentage of fibers in order to determine how well the OU J3 mix would withstand typical winter cycles a bridge would see, which is one of the main ways UHPC is used. In Figure 69 it can be seen that the specimens did not deteriorate during the test as the recorded test data of frequency increase over time. This increase in frequency indicates an increase in strength as the OU J3 specimens actually gained strength over the duration of the first 350 cycles due to being exposed to a moist environment which helped the concrete cure even further.

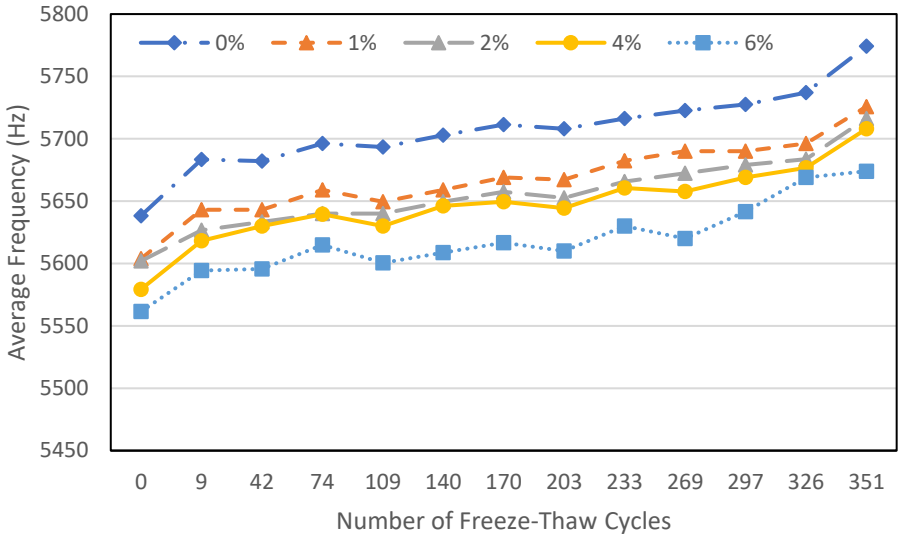

Figure 69: Freeze-thaw progression of average frequency over time

An increase in frequency also corresponds to an increase in relative dynamic modulus (RDM) as can be seen in Figure 70. Both plots show a general trend upwards with the specimens behaving in unison at each cycle they were tested. It seems that for both frequency and RDM analysis, for the majority of test cycles, if one percentage decreased or increased in measurement then the rest did too. Since the general trend is upwards, this variability from test day to test day can be attributed to the slight inconsistencies in testing procedure between different days. This variability of the test method could have come from the variation in the force used to hit the

specimens in order to record the frequency or the moisture content of the specimens between testing days.

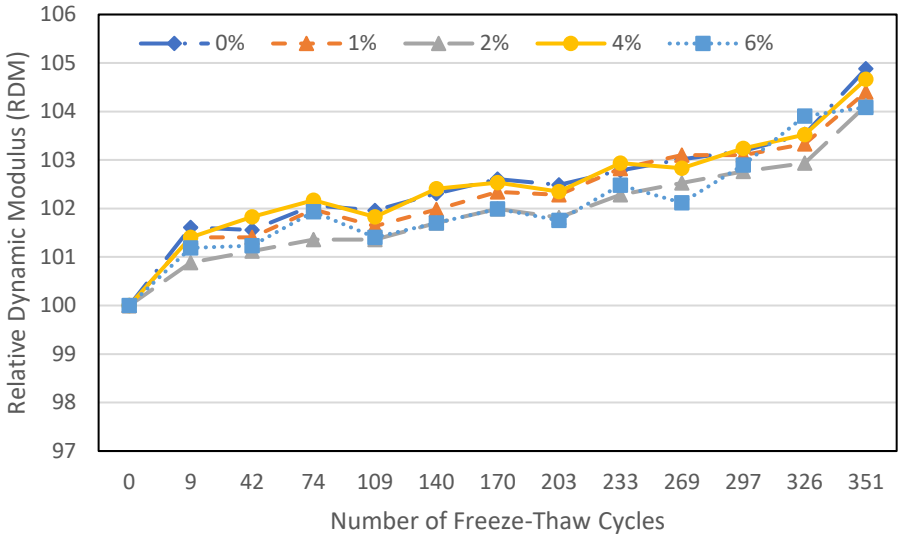

Figure 70: Freeze-thaw progression of relative dynamic modulus over time

Unlike typical concrete when exposed to the freezing and thawing cycles, the OU J3 freeze-thaw specimens underwent minimal visual physical change. In Figure 71 the specimens are shown at the end of the 14 day curing time at which the freeze-thaw test was started. The prisms have imperfections from the forms and spots of exposed fibers as has been typical when working with UHPC or OU J3 in particular. This is the visual starting point to which the observation from the rest of the test days was compared. Figures 72-74 show these specimens at the end of 351 freeze-thaw cycles. In general, there appears to be no significant notable change to the specimens besides rust at the exposed fibers especially if not inspecting them close up.

In Figure 75 a 2% specimen is shown which was observed to have formed rust after just 9 cycles in the freeze-thaw chamber at which time the first data was collected. These exposed fibers were the weakest point of all OU J3 specimens during this test.



Figure 71: Freeze-thaw specimens after 0 cycles (07/01)



Figure 72: Freeze-thaw specimens after 351 cycles (11/03 final day)



Figure 73: Close up view of freeze-thaw specimen ends after 351 cycles (11/03 final day)



Figure 74: Freeze-thaw specimens after 351 cycles (11/03 final day) showing rusted exposed fibers



Figure 75: Freeze-thaw first sign of rust on 2% specimen after 9 cycles (07/08)

A progression of this minimal deterioration of the same 6% specimen was captured in Figure 76. The furthest left picture shows this specimen at zero freeze-thaw cycles. Once again, many exposed fibers are visible around the edge of the top casting surface. This phenomenon got worse with increasing percentage of fibers and was less noticeable at lower fiber percentages. The middle picture in Figure 76 shows the 6% specimen after 42 cycles have been completed, this was the second time all the specimens were removed from the freeze-thaw chamber and tested. It can be observed that some rust has formed around the edges, but the specimen remained virtually the same. In the furthest right picture of Figure 76 the 6% specimen is shown after 351 cycles, this was the final time the specimens were retrieved from the freeze-thaw chamber. More rust appears to have formed along the exposed fibers and the specimen seems to have experienced minimal chipping along the top edges, otherwise it remained virtually the same and the weight measurements confirm this with most any of the ten freeze-thaw specimens losing being 0.03 lb over the course of 35 cycles. This minimal weight change can be confirmed

visually by inspecting the freeze-thaw chamber and the trays that held the specimens during testing. As can be seen in Figure 77, these trays have a minimal amount of chipped concrete in them. No significant chunks of concrete came off the specimens as the result of the freeze-thaw testing, nor did any notable physical changes occur besides rusting and slight accentuation of the imperfections on the cast surfaces.



Figure 76: Freeze-thaw 6% specimens after 0 (7/01) (left), 42 (7/15) (middle), and 351 cycles (11/03) (right)



Figure 77: Freeze-thaw chamber trays after 351 cycles (11/03 final day)

4.2 Florida International University (FIU) Materials J3 Mix

4.2.1 Flowability

The FIU J3 mix flow tests generally had a higher flow than the OU J3 mix which progressively decreased with increasing percentage of fibers as can be seen in Table 11. The concrete flowed off the table for the 0 and 1% fiber mixes (Figures 78 and 79), while the 2% fiber mix stayed within the limits of the flow table. The 4 and 6% fiber mixes experienced the same segregation between fibers and the rest of the concrete mixture (Figures 80 and 81) as in the OU J3 mix. The greatest difference between the results from the J3 mix made with materials from the two different universities was the amount of HRWR required. For the FIU J3 mix the HRWR content was increased to get the flow to be between 8 and 10 inches for all percentages of fibers (kept constant for 0, 1, and 2% and increased further for 4 and 6%), however even with the increase in HRWR, which resulted in a higher flow, the FIU J3 mix had a much shorter work

time. The FIU concrete mix was more fluid than the OU mix during and immediately after mixing, but within minutes became very stiff and lost most of its workability. Similarly to the OU mix, the fibers settled to the bottom for the 6% batch and the distribution of the fibers in the specimens was inconsistent. Fiber distribution in a given specimen was mostly based on where the concrete placed in the form was taken from – be that from the top or the bottom of the mixture in the transport container. It must also be noted that for the FIU J3 mixes the HRWR used was the same as for the freeze-thaw mixes but different than that used for the OU J3 mixes. Also, the slag that was used experienced potential moisture exposure during transport from FIU and instead of a powder consisted of very small balls formed from the fine powder. This most likely is what made the mixture more fluid upon mixing as there was less exposed surface area of the slag particles to absorb the moisture.

Table 11: FIU J3 flow test results

Percent Fibers (%)	**Flow (in)**	**HRWR (oz/cwt)**
0	10	23
1	9.75	23
2	9.25	23
4	8.5	25
6	5	30



Figure 78: FIU J3 0% fiber mix flow test



Figure 79: FIU J3 1% fiber mix flow test



Figure 80: FIU J3 4% fiber mix flow test



Figure 81: FIU J3 6% fiber mix flow test

4.1.2 Compressive Strength

The average compressive strength test results (three specimens each) for the FIU J3 mixes are listed in Tables 12 and 13 for all test days for both cylinders and cubes, respectively. The same data is further plotted in Figures 82 and 83. Similarly to the OU J3 cylinder specimens, the FIU J3 cylinder specimens did not experience a steady increase in compressive strength as depicted in Figure 82; there was a general increasing trend that appeared to level off with some fluctuation up and down at individual test results. Most notably, there was some fluctuation around the plateaued value for the 0, 2, and 4% fiber mix cylinders. For all three, the compressive strength decreased for 56 day testing as compared to the 28 day reading. It is probable that the strength gain simply plateaued between 28 day and 56 day testing and the results for the 56 day testing only indicate typical variation between compressive strength tests. Data for the individual specimens tested for each percentage of fibers can be found in Table 17 in Appendix C, which shows the range of values for the individual tests.

Table 12: FIU J3 cylinder compressive strength test data for each steel fiber content

Concrete Age (days)	**0%**	**1%**	**2%**	**4%**	**6%**
3	9,300	11,550	11,380	10,970	12,350
7	13,550	13,550	14,070	13,140	15,260
28	15,090	13,680	16,160	17,050	18,570
56	14,180	15,230	16,120	16,610	19,460

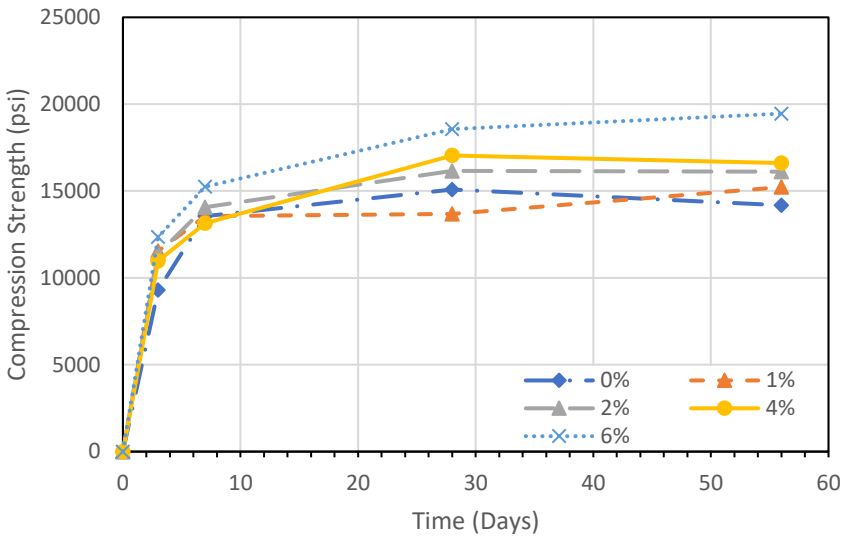

Figure 82: FIU J3 cylinder compressive strength test results

On the other hand, the cube specimen results exhibit consistent increase in compressive strength over time as can be seen in Figure 83, with the only notable data point being the close proximity of the 56 day results for the 2 and 4% fiber specimens. The similarity of the 2 and 4% fiber mix results is also captured in the cylinder data. This shows that the 2 and 4% fiber mixes have a very similar compressive strength with the 4% cylinders having a lower compressive strength at 3 and 7 days as can be seen in Table 12. Based on this data it can be said that increasing the fiber percentage from 2% to 4% did not significantly increase compressive strength as the 4% fiber mix closely matched the compressive properties of the 2% fiber mix.

Table 13: FIU J3 cube compressive strength test data for each steel fiber content

Concrete Age (days)	**0%**	**1%**	**2%**	**4%**	**6%**
3	8,071	9,308	12,125	12,711	12,454
7	9,034	10,895	14,320	15,412	16,109
28	10,910	14,362	16,626	17,860	19,549
56	11,847	15,969	19,290	19,701	20,939

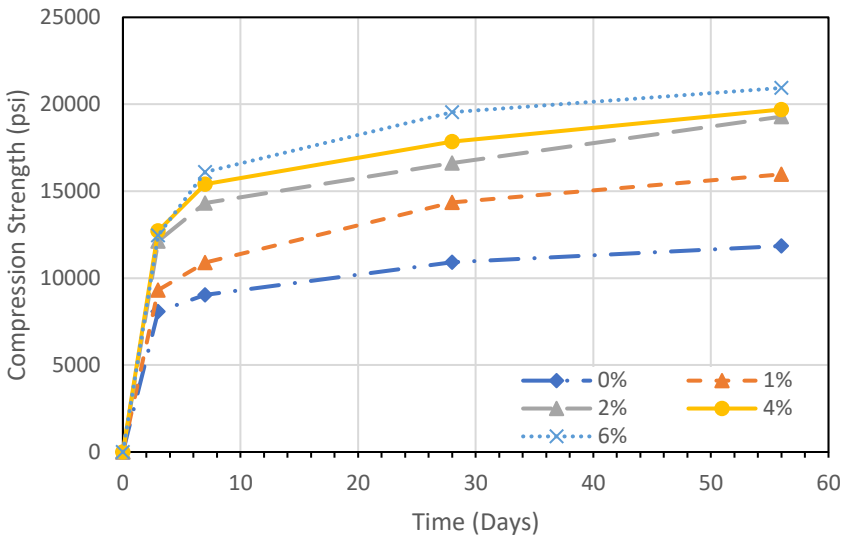

Figure 83: FIU J3 cube compressive strength test results

When comparing the data of all the 28 day cylinder compressive strength test results, which includes the OU J3, freeze-thaw, and FIU J3 specimens, it can be seen that the data has some inconsistencies. The FIU J3 data more closely resembles the trend of the OU J3 data rather than that of the freeze-thaw cylinders as can be seen in Table 14 and Figure 84. The other similarity between the FIU and OU J3 is the low compressive strength of the 1% fiber mix as compared to the 0% fiber mix at 28 days of age, which can also be seen in Figure 84. Based on this comparison the freeze-thaw cylinder compressive strength test results seem to be the outlier with the steady increase in strength with increase in percentage of fibers (Figure 84). Since only once batch was conducted for each fiber percentage, additional testing is needed to further investigate the anomaly seen for the 1% fiber mix. Figure 85 shows the comparison of FIU and OU J3 cylinders for 56 day testing for all percentages of fibers. This data shows a gradual increase in strength with an increase in fibers for FIU J3 mix, but the results for OU J3 mix remain inconsistent. It appears that for OU J3 the 6% had the highest compressive strength, followed by 2%, then 4%, then 1%, and finally 0%, but all results remained between 16900psi and 18400 psi, which is not a as large a spread compared to the FIU results (Figure 85). The cube

compression data was more consistent for both 28 day and 56 day testing windows (Figures 86 and 87). For both OU and FIU J3 mixes, the strength increased with increasing percentage of fibers with OU J3 notably having a smaller spread between the results for each percentage as compared to FIU cube results which underwent a greater gain in strength between each percentage of fibers.

Table 14:Comparison of OU J3, Freeze-thaw, and FIU J3 28 day cylinder compressive strength test results for each fiber content

Mix Type	**0%**	**1%**	**2%**	**4%**	**6%**
OU J3	16,380	13,250	17,220	17,490	17,510
Freeze-Thaw	12,440	12,890	13,700	15,010	16,630
FIU J3	15,087	13,678	16,160	17,045	18,570

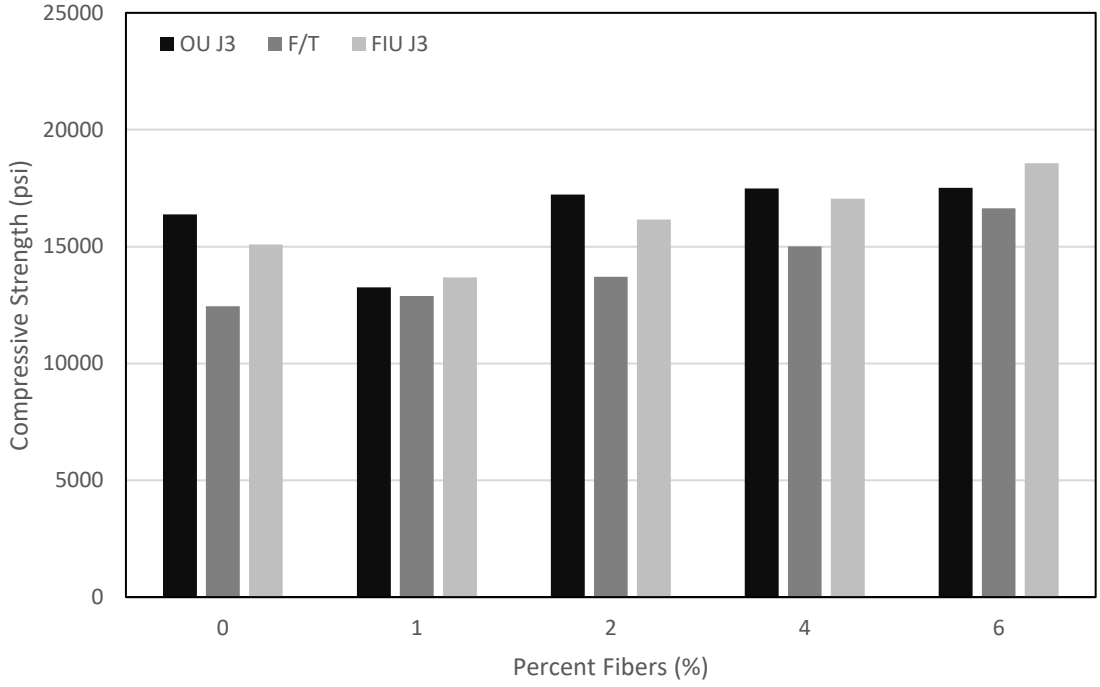

Figure 84: Comparison of OU J3, Freeze-thaw, and FIU J3 28 day cylinder compressive strength test results

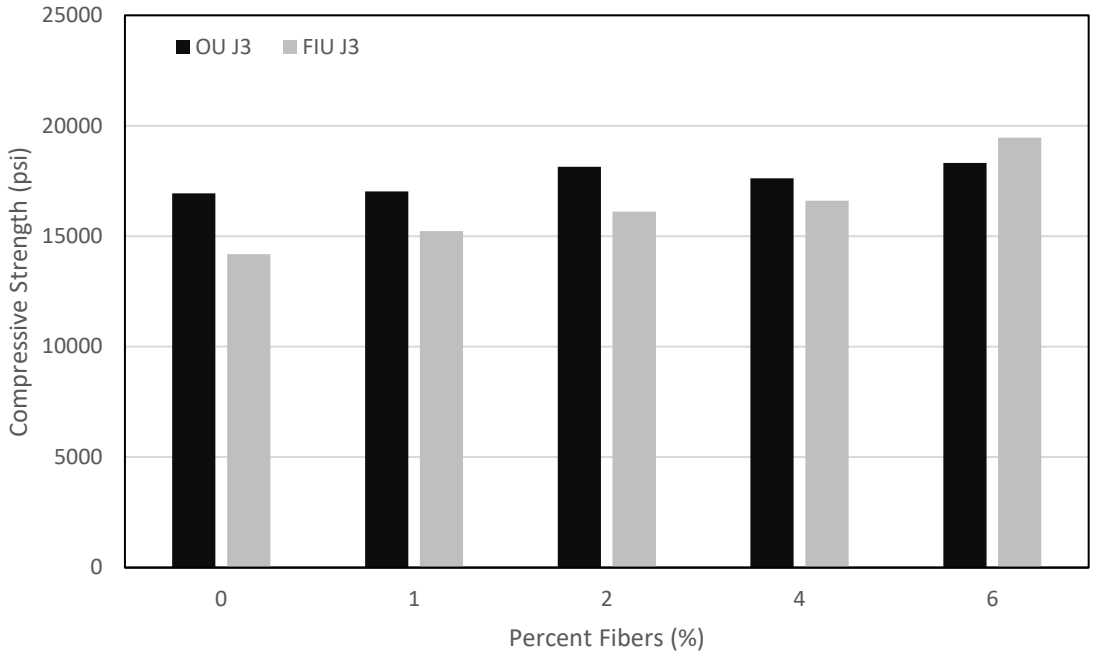

Figure 85: OU J3 vs. FIU J3 56 day cylinder compressive strength test results

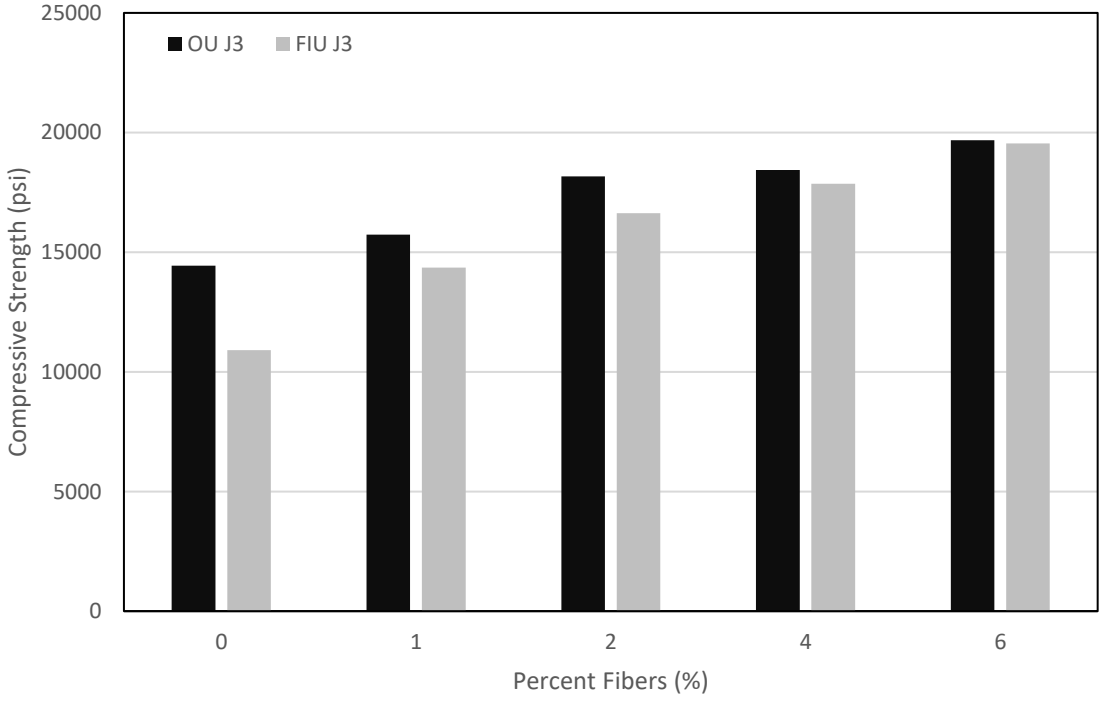

Figure 86: OU J3 vs. FIU J3 28 day cube compressive strength test results

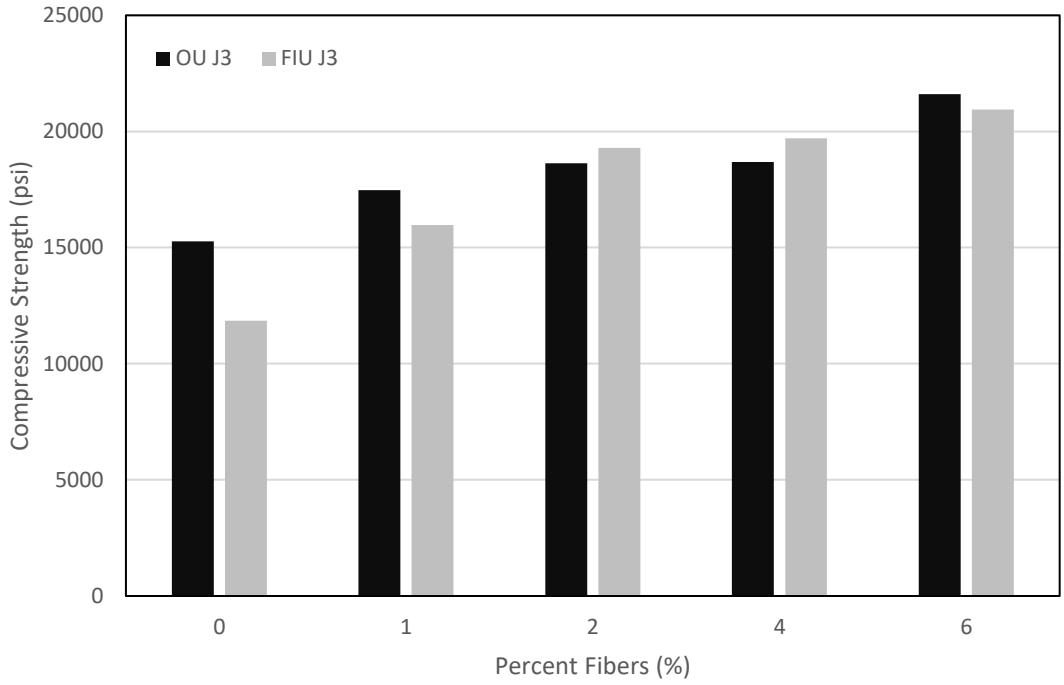

Figure 87: OU J3 vs. FIU J3 56 day cube compressive strength test results

It must be noted that only the 28 day compression cylinders were included in the FIU J3 discussion as the visual results were almost identical to the observations discussed earlier for the OU J3 specimens at various testing days.

Visually FIU J3 compression specimens underwent the same change upon failure as did the OU J3 and the freeze-thaw cylinders. The 0% specimen shattered under sudden failure (Figure 88), while with any amount of fibers the failure became gradual as the fibers held the specimen together under a higher load (Figures 89-92). Also, similarly to the aforementioned cylinder specimens, FIU J3 also experienced increasingly irregular cracks and more flaking with an increase in percentage of fibers. It appears that the 28 day 6% FIU J3 specimens experienced a significant amount of rusting not seen for the OU J3 and freeze-thaw 6% cylinders (visible in Figure 92), but this is likely due to the FIU J3 specimens having been ground prior to testing day and left to sit in the water tank with the steel fibers exposed. This should not have had any effect on the results.



Figure 88: FIU J3 0% cylinder 28 day compressive strength test specimens after failure



Figure 89: FIU J3 1% cylinder 28 day compressive strength test specimens after failure



Figure 90: FIU J3 2% cylinder 28 day compressive strength test specimens after failure



Figure 91: FIU J3 4% cylinder 28 day compressive strength test specimens after failure



Figure 92: FIU J3 6% cylinder 28 day compressive strength test specimens after failure

4.1.3 Flexural Strength/Modulus of Rupture

Similarly to the OU J3 specimens, the data from the FIU specimens shows a clear trend of increase in flexural tension strength (MOR) with increase in fiber percentage as can be seen in Table 15 and Figure 93. The presented data are averages of results for three or four individual specimens. Though unlike the OU J3 results, the 4% and the 6% fiber specimens follow the overall trend. This continuous trend is what was expected and based on this and the results shown in Figure 93 it seems the lower MOR values seen for the OU J3 6% fiber mix was a bit of an outlier either due to the variation of sources for materials as compared to the FIU J3 or due to the low flow of the OU mix. As discussed earlier, the low flow of the 6% fiber mix could have led to settling of the fibers and their segregation from the mixture sometime shortly after completion of the mixing and thus to a lower overall strength. But it must also be noted that the very high results for the 4% OU J3 specimens were also likely an outlier as discussed previously.

Additionally, Figure 93 shows that the specimens tested at 56 days performed better than the specimens tested at 28 days for every fiber percentage and the strength increased as the percentage of fibers increased being the most significant for 4% specimens. The increase between 28 and 56 days for 0% was 121 psi or 7%, for 1% it was 246 psi or 13%, for 2% it was 312 psi or 13%, for 4% it was 476 psi or 13%, and for 6% it was 326 psi or 8%; thus, the average increase is 11%. This is similar the OU J3 results where there was no consistent trend associated with the percentage increase, though the average is a third of the 29% increase found for the OU J3 specimens. There also appears to be a very small difference in flexural strength between the 0 and 1% fiber specimens, the increase from one to another for 28 days is only 5% and for 56 days it is only a little bit higher at 11% increase. For the OU J3 mix the increase in flexural strength between 0 and 1% was 40% for 28 days and 42% for 56 days. Data for the individual specimens tested for each percentage of fibers is shown in Table 19 in Appendix C, which shows the range of values.

Table 15: OU J3 vs. FIU J3 flexural strength (MOR) for each steel fiber content

Type	Concrete Age (days)	0%	1%	2%	4%	6%
OU J3	**28**	1,265	1,765	2,450	4,280	3,560
	56	1,735	2,470	3,040	4,140	4,140
FIU J3	**28**	1,840	1,935	2,490	3,590	4,160
	56	1,960	2,180	2,800	4,065	4,490

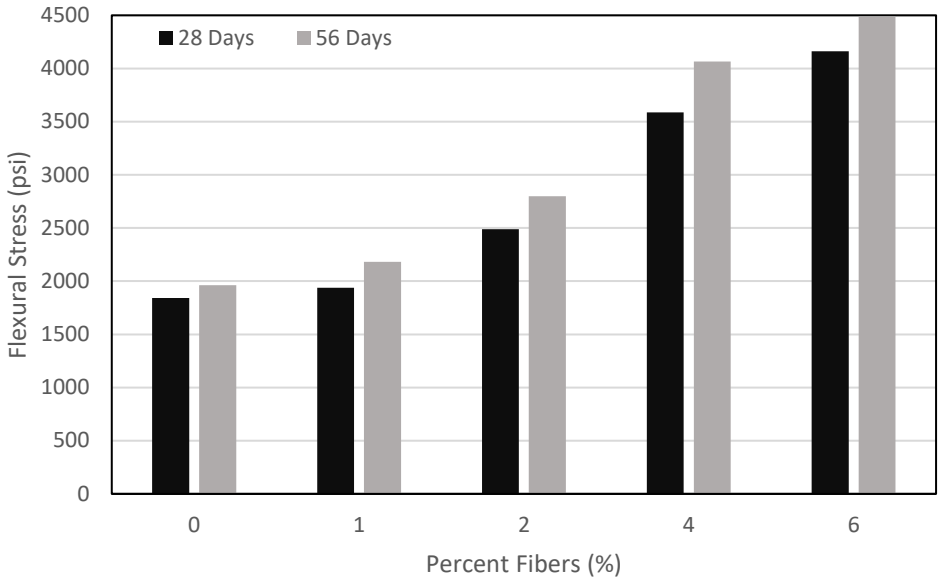

Figure 93: FIU J3 MOR maximum strength 28 vs 56 day

Figure 94 shows a further comparison of the MOR results at 28 and 56 days for both OU J3 and FIU J3 specimens. Based on this graph some interesting trends can be seen, but there is not enough data to fully establish which mix exhibited better performance or if the performance was equivalent. It appears that OU J3 outperformed FIU J3 for 4% fiber mix for both 28 and 56 days, but FIU J3 performed better for the 0 and 6% fiber mixes at both ages tested. Meanwhile, the 1 and 2% fiber mixes exhibited split results with FIU J3 performing better at 28 days and OU J3 performing better at 56 days. The 28 day comparisons for OU and FIU J3 and 56 day comparison are also shown separately in Figure 95 and Figure 96 respectably. More testing is required for a proper conclusion especially in regards to 4 and 6% mixes for OU J3.

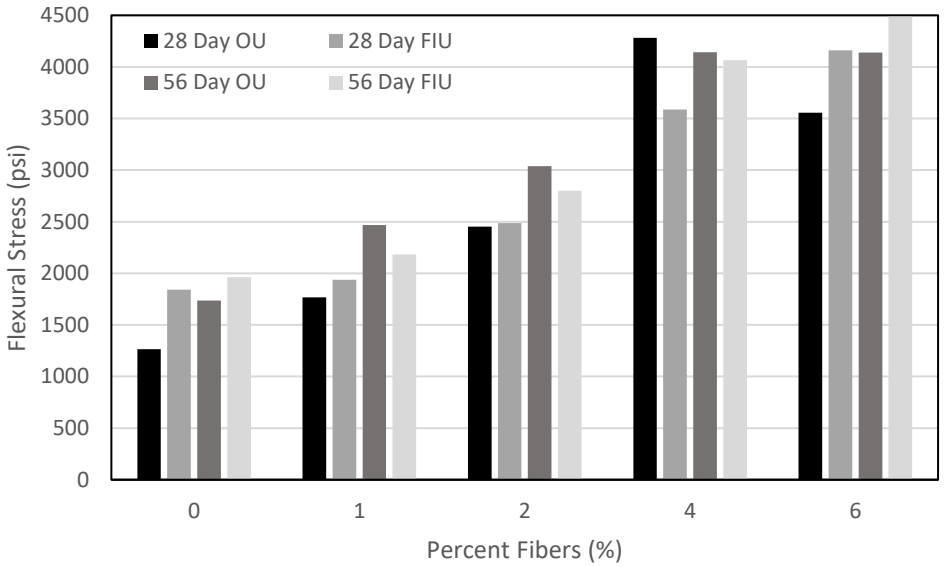

Figure 94: OU vs. FIU J3 MOR results at 28 days and 56 days

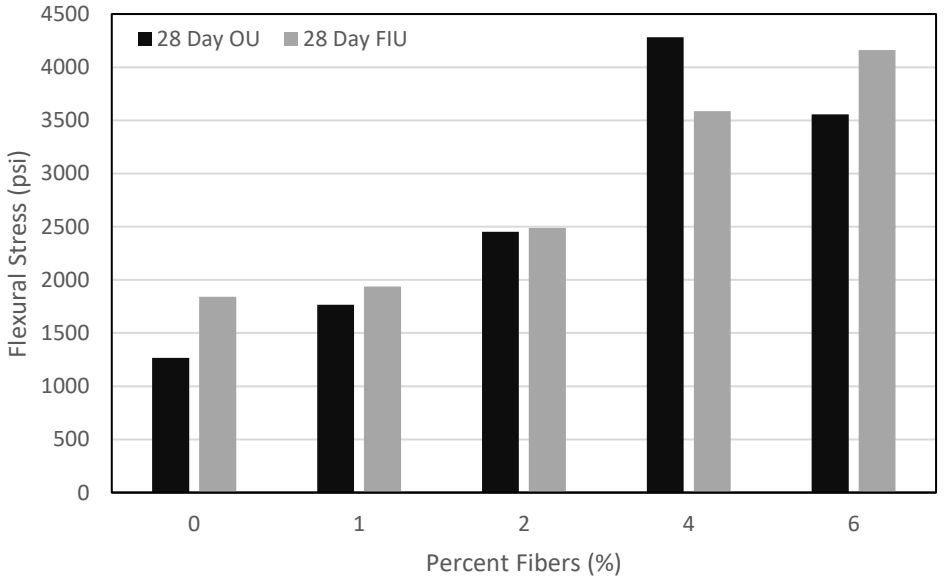

Figure 95: OU vs. FIU J3 MOR results at 28 days

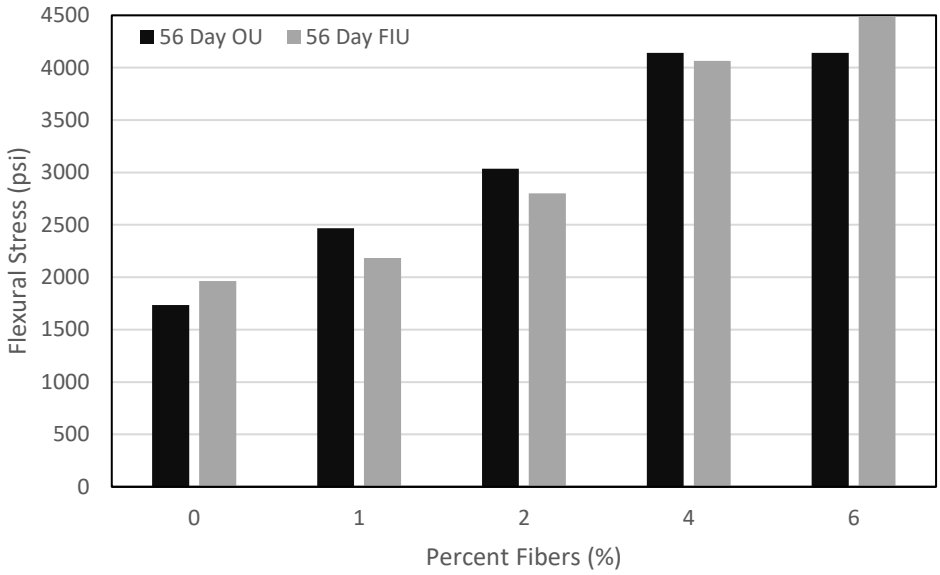

Figure 96: OU vs. FIU J3 MOR results at 56 days

Just like with the OU J3 specimens, the flexural stress multiplier determined by dividing each result by the square root of the measured compressive strength was considered in the analysis of the FIU J3 specimens. Looking at Figure 97, it can be seen that it largely mimics the comparison of the non-normalized MOR values Figure 93, though with the value for 28 and 56 days being much closer together.

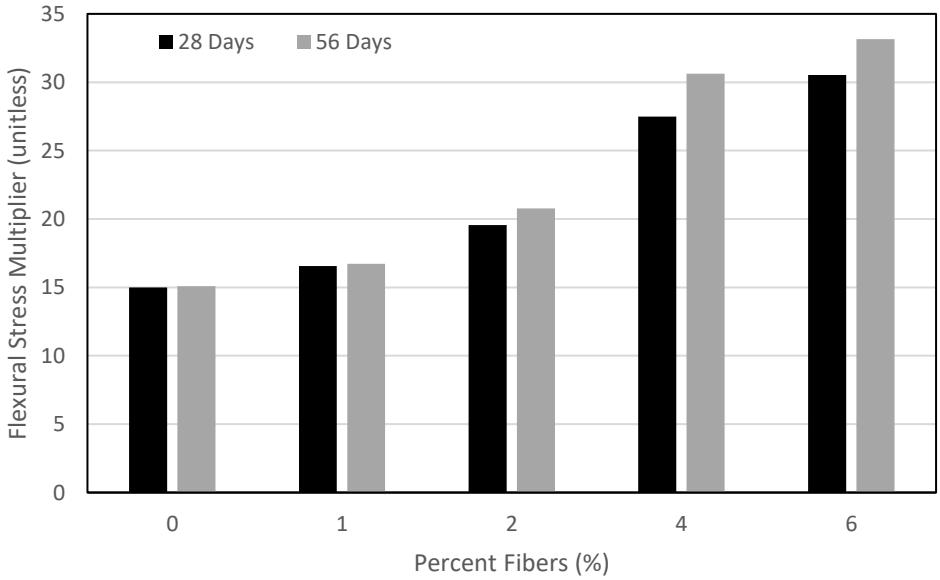

Figure 97: FIU J3 MOR results normalized by square root of compressive strength

Alternatively, the MOR results normalized by compressive strength are also represented in Figure 98 where a more concise overall comparison for both OU and FIU mixes is shown for both testing windows.

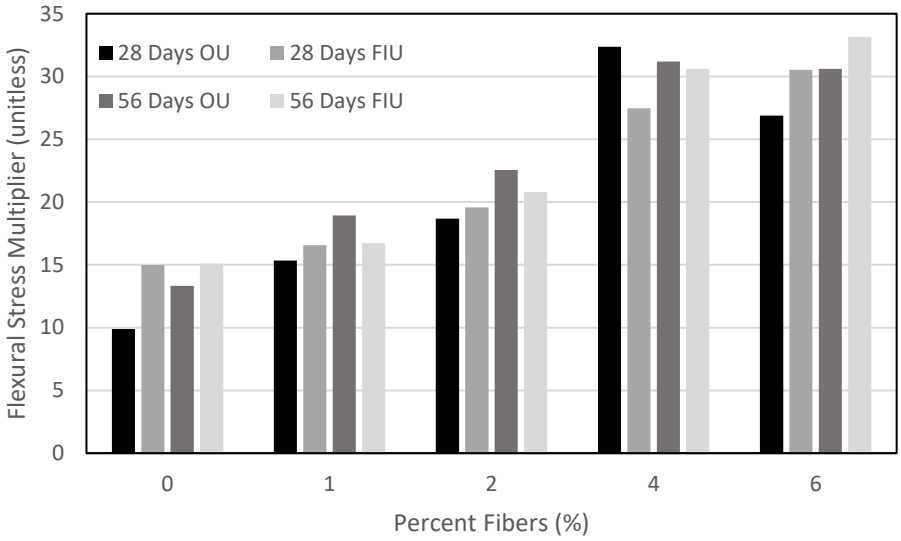

Figure 98: OU and FIU J3 MOR results normalized by square root of compressive strength for 28 and 56 days

Visually the FIU specimens were very similar to the OU specimens after failure. The 0% fiber mix experienced a clean sudden break, while with any fiber percentage the specimen stayed in one piece and experienced slow failure as the beam cracked. The crack pattern was mostly vertical or diagonal (Figure 101) and became more of an irregular pattern with the increase in fiber percentage (Figures 102-104). This is most likely due to the fibers creating resistance to the crack developing a clear path, and thus following the path of least resistance and navigating to the weaker areas of the specimen. Two of the specimens for the 28 day testing developed a fracture outside of the middle third of the span (first 2% fiber specimen and first 4% fiber specimen) and so did one specimen for the 56 day testing (first 6% fiber specimen). The 6% fiber 56 day specimen, more precisely, cracked outside of the allowable fracture region which can be

no more than 5 % of the span length outside of the middle third, therefore the results for this test were discarded though the picture is still included in Figure 109 for reference. Since only three prism specimens were cast for each percentage of the FIU J3 mix, there was no extra specimen to rerun the test, thus the data given above is an average of two specimens.

Besides these two occurrences, one of the 2% fiber specimens tested at 56 days developed two very similar cracks. These cracks developed right on the outside boundaries of the marked middle third section (Figure 107). There is no equation provided in ASTM C78 to address this scenario and there were no extra specimens to run an additional test to ensure the strength of that specimen was not an outlier. This test was not discarded, but all measurements were made to the larger of the two cracks. It must be noted that the maximum load for this specimen was approximately 1600 lb or 20% higher than the next highest strength specimen out of the three tested. The test results were as follows 9940 lb, 8260 lb, and 7500 lb with the specimen with two cracks having the highest load at failure.



Figure 99: FIU J3 0% 28 day MOR test specimens after failure

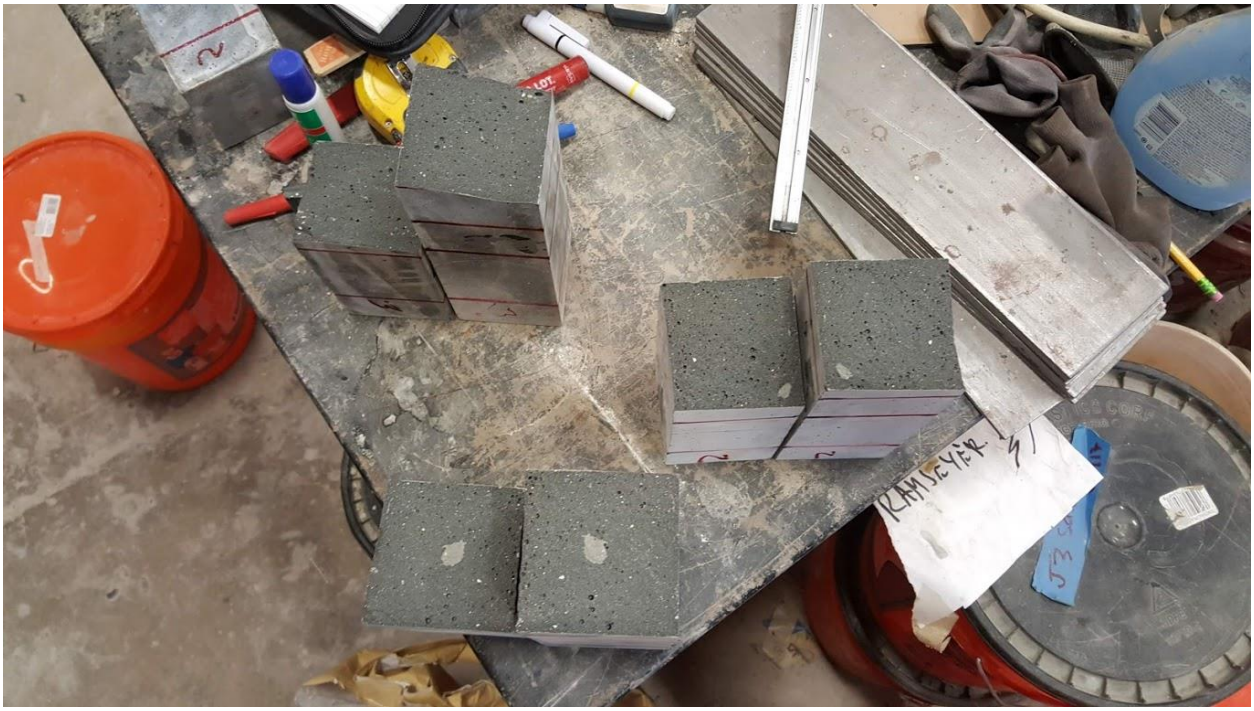

Figure 100: FIU J3 0% 28 day MOR test specimen cross section



Figure 101: FIU J3 1% 28 day MOR test specimens after failure



Figure 102: FIU J3 2% 28 day MOR test specimens after failure



Figure 103: FIU J3 4% 28 day MOR test specimens after failure



Figure 104: FIU J3 6% 28 day MOR test specimens after failure



Figure 105: FIU J3 0% 56 day MOR test specimens after failure



Figure 106: FIU J3 1% 56 day MOR test specimens after failure



Figure 107: FIU J3 2% 56 day MOR test specimens after failure



Figure 108: FIU J3 4% 56 day MOR test specimens after failure



Figure 109: FIU J3 6% 56 day MOR test specimens after failure

Additionally, the data recorded from the LVDT during each test was used to create load vs. deflection curves for each percentage of fibers in order to observe the specimens post-cracking behavior. For the following representative curves seen in Figures 109-114 only the 28 day specimens from the FIU J3 mix were used. The second out of three MOR specimens was used for most of the graphs, but this was not possible so for the 4 and 6% fiber mixes the third specimen out of the three tested was used. The 0% fiber specimen performed as would be expected of any unreinforced concrete and, as seen in Figure 109, underwent sudden failure after it reached its maximum strength. On the other hand, the 1, 2, 4, and 6% fiber specimens continued to take on greater load even after the first crack appeared, thus the maximum load occurred in the post-cracking region. In Figures 110 and 111 for 1 and 2% fiber specimens respectively, the cracking point is clearly visible at the very beginning of the graph after a steep, nearly linear portion. The load that the specimen is able to take on quickly drops before

increasing back up to the previous load, then reaching the maximum load used in the flexural strength analysis described above. The sharp drop in load is a function of the load control method used for loading the specimens. For the 4% fiber specimen the cracking point is less clear when looking at Figure 113. If looking closely there seems to be an imperfection in the graph between 5000 and 6000 lb at the very beginning, which could indicate the first crack. The load then once again increases reaching its maximum before the specimen cracks further and the load takes a small gradual dip before recovering once again but not to the full previously established maximum load. The 6% fiber specimen does not appear to be affected at all by the cracking as there is no sudden drop anywhere in the graph as for the other percentages. In fact, looking at Figure 114, it appears that the specimen reaches its maximum load after major cracking occurs. Finally, Figure 115 shows all of the load vs. deflection curves that were previously discussed in one graph. In comparison to each other it makes sense that the 6% fiber specimen has the greatest maximum load with 4% following underneath and then 2%, 1%, and finally 0%.

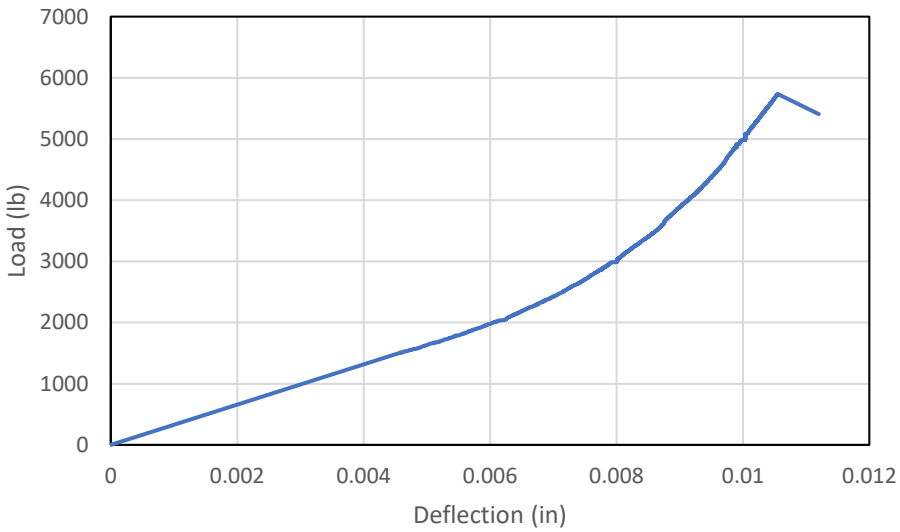

Figure 110: FIU J3 0% 28 day MOR test load vs. deflection curve

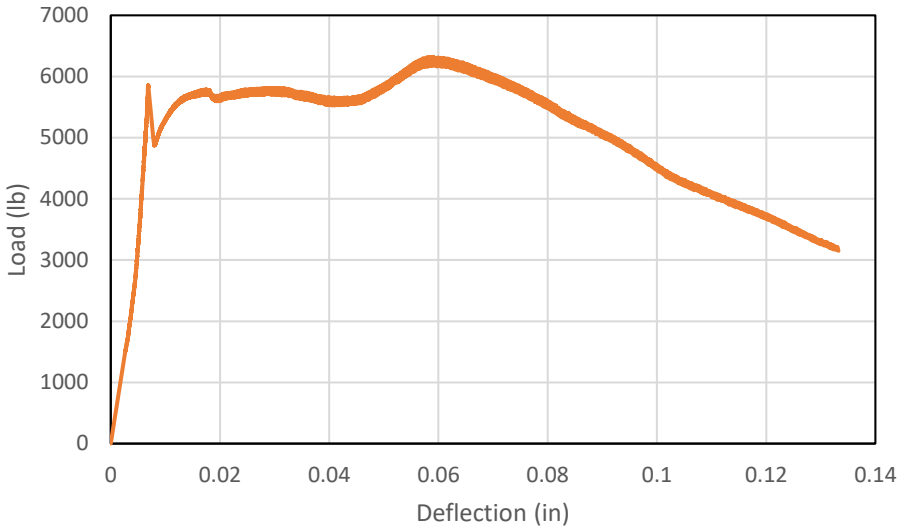

Figure 111: FIU J3 1% 28 day MOR test load vs. deflection curve

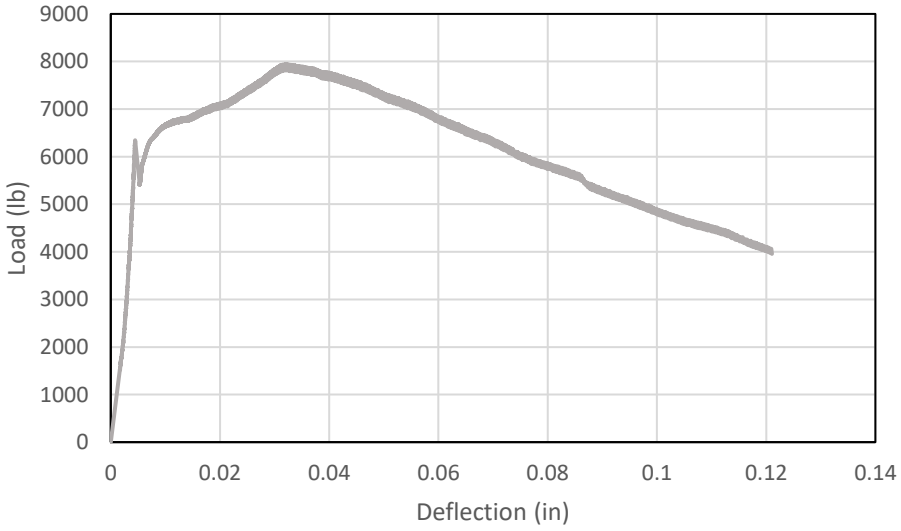

Figure 112: FIU J3 2% 28 day MOR test load vs. deflection curve

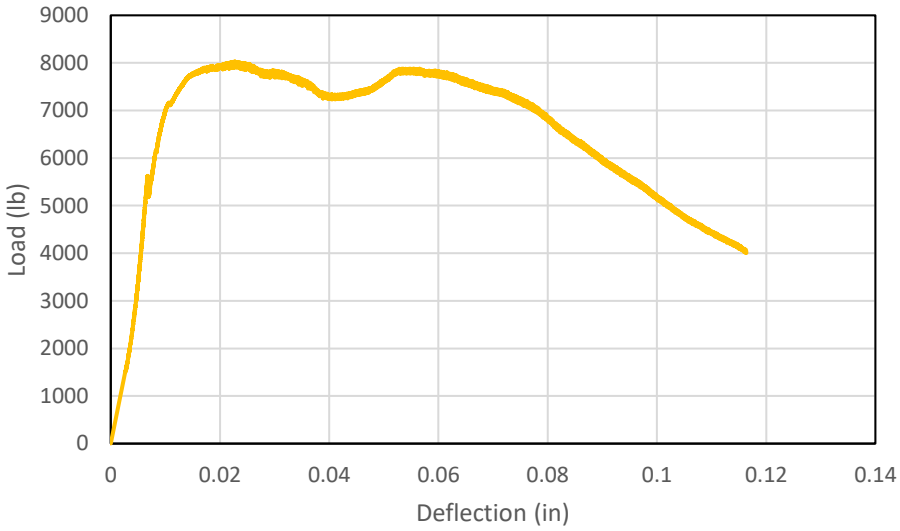

Figure 113: FIU J3 4% 28 day MOR test load vs. deflection curve

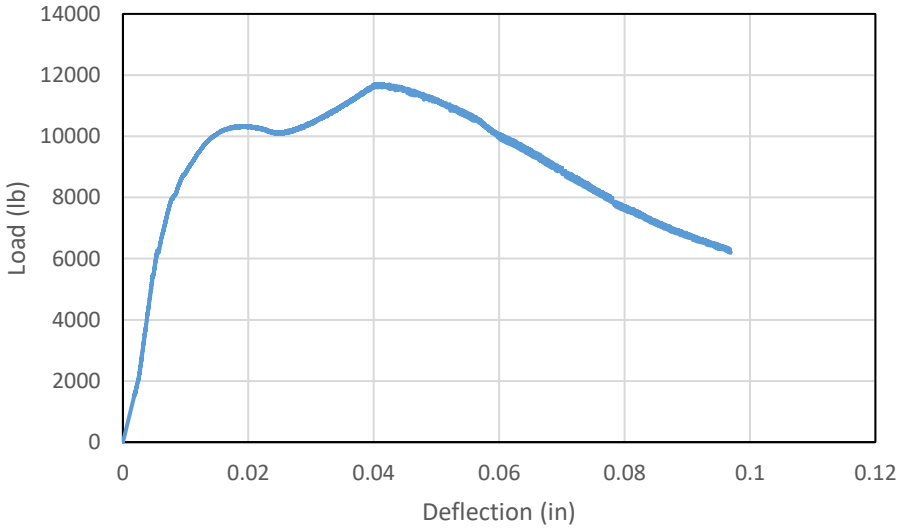

Figure 114: FIU J3 6% 28 day MOR test load vs. deflection curve

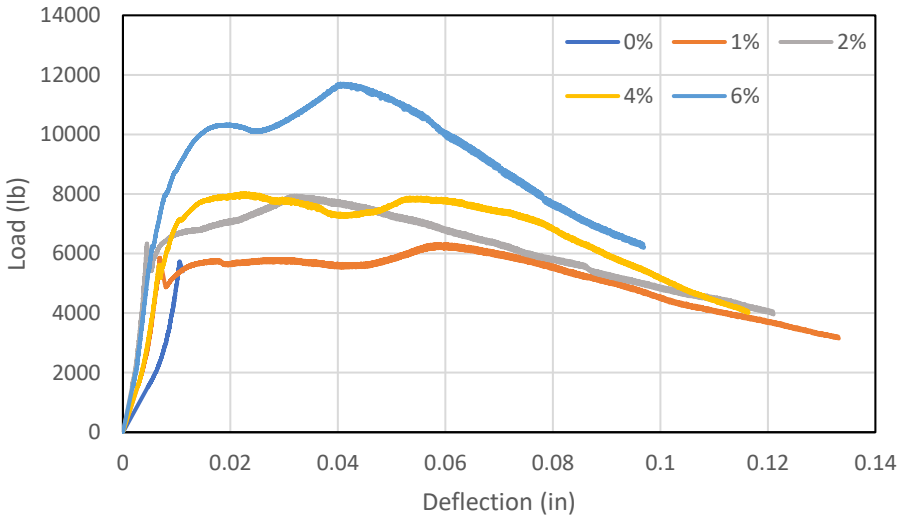

Figure 115: FIU J3 28 day test load vs. deflection curve for all fiber percentages

Chapter 5: Summary, Conclusions, and Recommendations

5.1 Summary

Two variations of the J3 UHPC mix developed at OU (Looney et al. 2019) were tested as part of the research described in this thesis. The first used materials locally available in Oklahoma and underwent flowability, compressive, modulus of elasticity (MOE), split cylinder, flexural, and freeze-thaw testing. The second used materials locally available in south Florida, near Florida International University (FIU), and was tested for flowability, compressive strength, and flexural strength. Each variation of the mix was tested with 0, 1, 2, 4, and 6% steel fibers by volume to determine their effect on the mechanical properties of the J3 mix. The results for each test were recorded and analyzed to determine how the percentage of steel fibers affect properties of the J3 mix and examined the repeatability of the mix by comparing the variations to each other at each percentage of fibers. The following conclusions are based on limited data and are generally only applicable to similar situations and user characteristics. It is possible that these conclusions would be altered if additional specimens were tested providing more data for in-depth statistical analyses.

5.2 Conclusions

Upon extensively testing the J3 UHPC mix it was determined that it performed quite well regardless of the location (OU vs. FIU) of where some of the materials were acquired and its performance improved with increasing percentage of fibers by volume. More specifically, the first version of J3 tested was identified as OU J3, which used local sources to Oklahoma for three materials – sand, slag, and cement. Specific conclusions related to the OU J3 mix are as follows:

- Results of the flowability test indicate lower workability for the 4 and 6% fiber mixes as neither was able to reach a desired flow of 8 in. or higher even with an

adjusted amount of HRWR. This is due to the high volume of fibers within the mix, which impede flow. The reduced workability also led to segregation of the concrete mixture as fibers would settle at the bottom of the molds, which would lead to uneven distribution of strength upon testing. The lower flowability also increased the chance for air bubbles getting trapped within the mix upon casting, which could have reduced strength during further testing. All these effects were more significant for the 6% fiber mix compared to the 4% steel fiber mix.

- Results of compressive strength testing revealed that fibers were beneficial in preventing sudden failure and crumbling of the concrete, but it appears that they had only contributed a small increase in compressive strength when looking at the cylinder specimens. With the cube specimens, a greater impact was noticeable, but while the strength increased by 36% from 0% to 6% steel fibers at 28 days, it would not be recommended to cast any specimens with more than 2% fibers as the increase in strength between the 0% and 2% fiber mixes for 28 days was 26%. Additionally, the 2 and 4% fiber specimens were almost identical in compressive strength for both cubes and cylinders.
- The modulus of elasticity gradually increased with increase in fibers.
- The splitting tensile test indicated that the concrete became much stronger in tension with any amount of fibers in the mix, though this increase was not as significant beyond 4% steel fibers.
- Flexural strength (modulus of rupture) results supported increasing tensile strength with increasing steel fibers and revealed that specimens with fibers were

able to reach maximum load after the specimen had already cracked, though this is discussed in more detail in relation to the FIU specimens.

- Finally, the freeze-thaw test revealed that the specimens remained unaffected by the freezing and thawing cycles and in fact gained strength during testing for all fiber percentages.

The second version of J3 tested was called FIU J3 and it used sources local to Florida for three materials – sand, slag, and cement. Specific conclusions related to the FIU J3 mix are as follows:

- The flowability test indicated a small increase in flow as compared to the OU J3 results. While the FIU J3 had more flow right after mixing, it also required more HRWR for all fiber percent mixes and lost workability faster than the OU J3 mix. The 6% fiber mix was the only one unable to reach the 8 in. flow even with an additional increase in HRWR.
- FIU J3 performed similarly to OU J3 during compressive and flexural strength testing with the only major difference being a significant compressive strength increase for the 6% fiber cylinder specimens at 28 days.
- It must also be noted that for both OU and FIU J3 mixes the 1% fiber 28 day cylinder compression specimens for an unexplainable reason decreased in strength or did not increase as much as expected as compared to its 7 day strength.
- In flexural strength testing the FIU J3 slightly outperformed the OU version for 28 day testing though the rest of the results were similar, showing an increase of flexural strength with increase in fiber percentage and curing time. By plotting the load vs. deflection curves, the results revealed that the 0% fiber specimens

underwent sudden failure upon reaching maximum load. The 1 and 2% fiber specimens exhibited a sudden drop in load upon appearance of the first crack but then were able to take on more load and reach maximum load post cracking, though the 1% mix did not see a significant increase in maximum load as compared to 0%. The 4 and 6% fiber mixes experienced a smoother drop in load over time before rebounding back to higher load and once again reaching maximum load post cracking. The 2 and 4% fiber mixes had similar results, while the 6% fiber mix had the highest flexural strength.

Overall, the research described in this thesis found that the non-proprietary UHPC J3 exhibited excellent performance under a variety of material property tests. An increase in fibers resulted in higher compressive and tensile strengths, but with diminishing returns. It was also found that J3 achieves most of its full strength within the first 28 days of curing and while some of the results were even higher for 56 days, some specimens appeared to have plateaued at that point.

5.3 Recommendations

Based on the results of the research described in this thesis the following recommendations are made:

- Fibers are an expensive component of the overall mixture, thus, unless the absolute maximum strength is required and depending on the applications, using 6% should be avoided. Using 2 or 4% should provide better workability and most optimal strength from fibers.
- Additional characterization of the constituent materials is needed (particle size, particle shape, chemical composition, and reactivity), especially for those obtained from FIU, in

order to better understand differences and similarities in performance between the two mixes.

- Compression and freeze-thaw tests revealed that the J3 mix remained strong regardless of the percentage of fibers, and minimal gains in strength were seen with increase in fiber though they did prevent sudden failure. Percentage of fibers only had a major effect when the specimen was under tension and in this case the increase in fibers caused an increase in strength. It would be recommended to only pursue higher percentages of fibers for J3 when tension strength is a major concern and rely on the 1% fiber mix otherwise.
- Additional compressive strength testing is recommended for all percentage of fibers cylinders using the same Forney machine, especially focusing on the 1% mix.
- Additional flexural strength (modulus of rupture) testing is recommended for the OU J3 mix at 4 and 6% fibers.
- Optimization of the 6% mix for flowability is necessary prior to more testing being done. Due to excessive segregation of fibers, it is not certain whether the results described are fully representative of the material behavior. More testing with a higher amount of HRWR is recommended.

References

1. Haber, Z. B., De la Varga, I., Graybeal, B. A., Nakashoji, B., and El-Helou, R. “Properties and Behavior of UHPC-Class Materials,” Report No. FHWA-HRT-18-036, Federal Highway Administration, McLean, VA, 2018.
2. El-Tawil, S., Tai, Y. S., Meng, B., Hansen, W., and Liu, Z.. “Commercial Production of Non-Proprietary Ultra High Performance Concrete,” Report No. RC-1670. Michigan Department of Transportation, Lansing, MI, 2018, www.michigan.gov/documents/mdot/SPR-1670-2019_644044_7.pdf.
3. El-Tawil, S., Alkaysi, M., Naaman, A. E., Hansen, W. and Liu, Z. “Development, Characterization and Applications of a Non Proprietary Ultra High Performance Concrete for Highway Bridges,” Report No. RC-1637, Michigan Department of Transportation, Lansing, MI, 2016, www.michigan.gov/mdot/0%2C4616%2C7-151-9622_11045_24249_76865_76873-386988--%2C00.htm.
4. Graybeal, B. “Structural Behavior of Ultra-High Performance Concrete Prestressed I-Girders,” Report No. FHWA-HRT-06-115, Federal Highway Administration, McLean, VA, 2006.
5. Graybeal, B.. “Behavior of Field-Cast Ultra-High Performance Concrete Bridge Deck Connections Under Cyclic and Static Structural Loading,” Report No. FHWA-HRT-11-023, Federal Highway Administration, McLean, VA, 2010.
6. Le Hoang, A. and Fehling, E. “Influence of Steel Fiber Content And Aspect Ratio on The Uniaxial Tensile And Compressive Behavior of Ultra High Performance Concrete,” *Construction and Building Materials*, v. 153, p. 790-806, October 30, 2017, DOI: 10.1016/j.conbuildmat.2017.07.130.

7. Shehab El-Din, H. K., Mohamed, H. A., El-Hak Khater, M., and Ahmed, S. “Effect of Steel Fibers on Behavior of Ultra High Performance Concrete,” First International Symposium on UHPC, Des Moines, IA, July 18-20 2016, www.extension.iastate.edu/registration/events/UHPCPapers/UHPC_ID11.pdf.
8. “Ultra-High Performance Concrete.” Federal Highway Administration, U.S. Department of Transportation, 29 Aug. 2018, highways.dot.gov/bridges-and-structure/ultra-high-performance-concrete/ultra-high-performance-concrete.
9. “Ultra-High Performance Concrete.” PCA, Portland Cement Association, www.cement.org/learn/concrete-technology/concrete-design-production/ultra-high-performance-concrete.
10. Waidelich, W. C. “Ultra High Performance Concrete (UHPC) - Availability of Domestic Source of Steel Fiber Reinforcement and Proprietary Product Concerns.” Federal Highway Administration, U.S. Department of Transportation, 12 Feb. 2014, www.fhwa.dot.gov/construction/contracts/140212.cfm.
11. Wu, Zemei, Shi, C., He, W., and Wu, L. “Effects Of Steel Fiber Content And Shape on Mechanical Properties of Ultra-High Performance Concrete,” *Construction and Building Materials*, v 103, p 8-14, January 30, 2016, DOI: 10.1016/j.conbuildmat.2015.11.028.
12. Looney, T., McDaniel, A., Volz, J. and Floyd, R. “Development and Characterization of Ultra-High Performance Concrete with Slag Cement for Use as Bridge Joint Material,” *British Journal of Civil and Architecture Engineering*, v 01, no 2, September 2019..

Appendix A: Compressive Strength Specimens



Figure 116: OU J3 0% cube 3 day compressive strength test specimens after failure



Figure 117: OU J3 0% cube 56 day compressive strength test specimens after failure



Figure 118: OU J3 1% cylinder 3 day compressive strength test specimens after failure



Figure 119: OU J3 1% cylinder 7 day compressive strength test specimens after failure



Figure 120: OU J3 1% cylinder 56 day compressive strength test specimens after failure

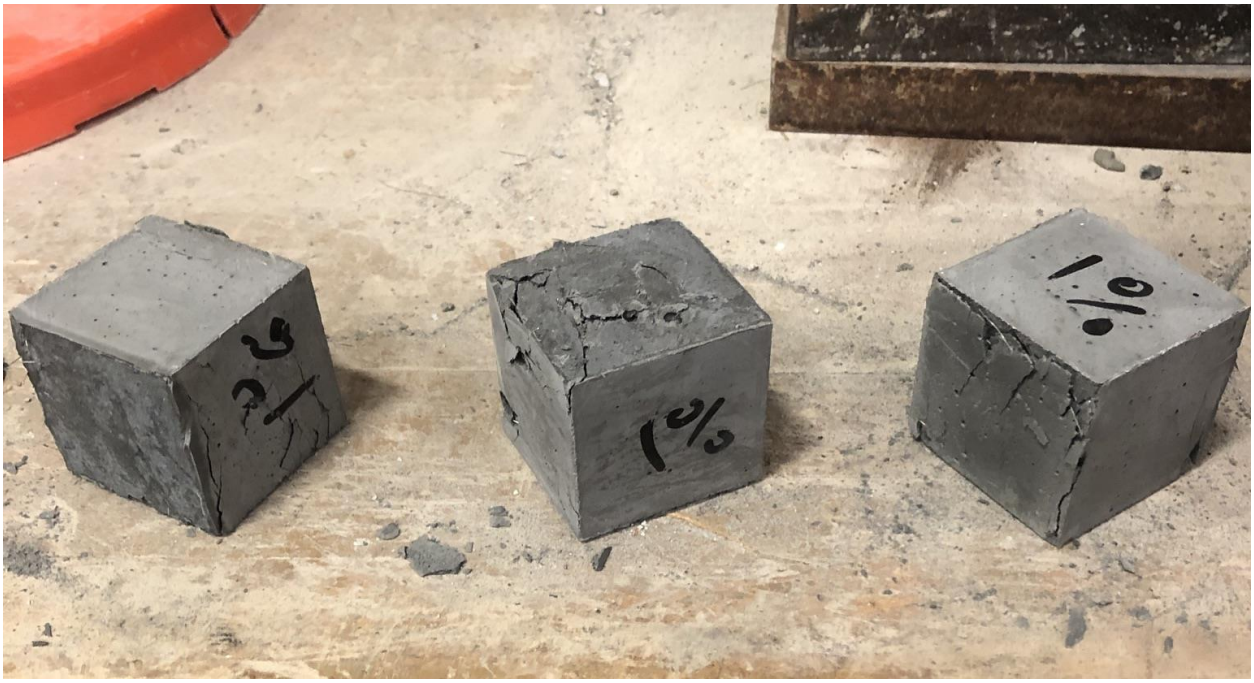

Figure 121: OU J3 1% cube 3 day compressive strength test specimens after failure



Figure 122: OU J3 2% cylinder 3 day compressive strength test specimens after failure

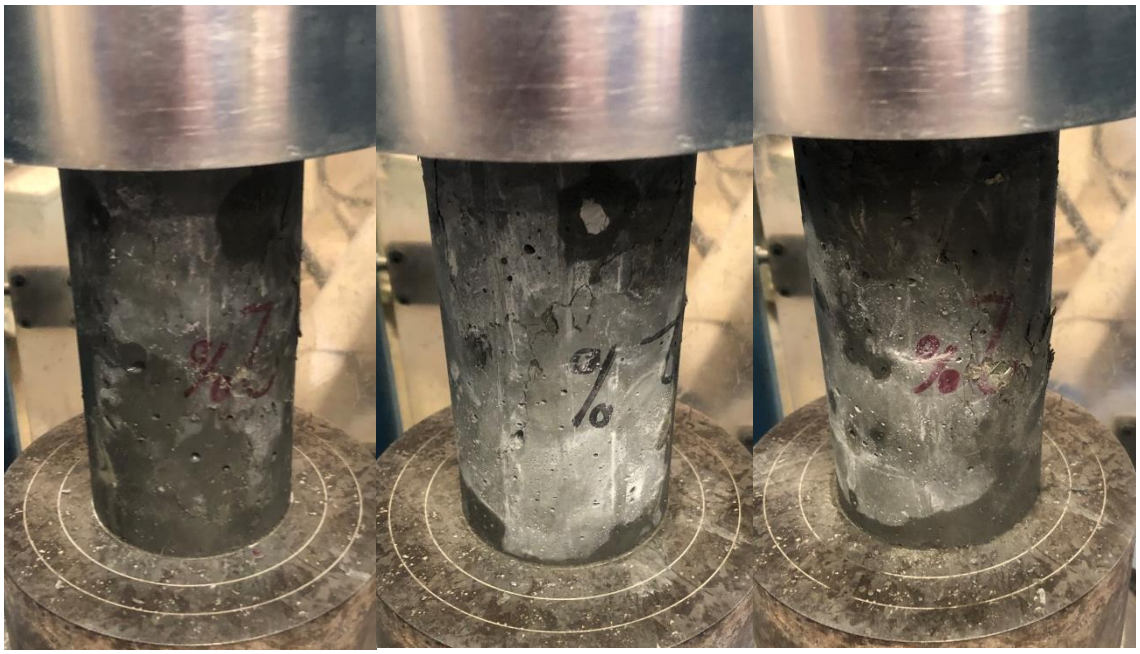

Figure 123: OU J3 2% cylinder 7 day compressive strength test specimens after failure



Figure 124: OU J3 2% cube 3 day compressive strength test specimens after failure

Appendix B: Constituent Material Information

Table 16: OU J3 and FIU J3 mix component information

	Material	Specific Gravity	Supplier
OU J3	Type I Cement	3.15	Ash Grove Chanute, Kansas
	Slag	2.97	Holcim, South Chicago
	Silica Fume	2.22	Norchem, Ohio
	Fine Masonry Sand	2.63	Metro Materials Norman, Oklahoma
	Steel Fibers	7.85	Bekaert (Dramix® OL 13/0.2)
	Superplasticizer	1.07	BASF (Glenium 7920)
FIU J3	Type I Cement	3.15	Titan America, Florida
	Slag Cement	—	Argos USA, Tampa, FL
	Silica Fume	2.22	Norchem, Ohio
	Silica Sand	2.64	Titan America, Florida
	Steel Fibers	7.85	Bekaert (Dramix® OL 13/0.2)
	Superplasticizer	1.07	BASF (Glenium 7920)

Appendix C: Individual Specimen Data

Table 17: OU J3 and FIU J3 compressive strength (psi) for each individual cylinder specimen for each steel fiber content

Mix	Age	0%	1%	2%	4%	6%
OU J3	3 days	12140	12305	12430	11095	12541
		12620	12050	12847	12338	12194
		13000	12154	12342	12107	12656
	7 days	13241	12890	14651	14611	15237
		13118	13807	14463	14408	14314
		13359	13537	14321	14488	14902
	28 days	15867	13051	17996	17403	16744
		16112	11176	15868	17793	18353
		17157	15521	17792	17274	17423
	56 days	16119	16222	18889	17625	18745
		17313	16839	18161	16952	17895
		17400	18011	17384	18288	18305
Freeze-thaw	28 days	12575	12330	13560	14745	16275
		12260	13320	14180	14845	16850
		12475	13005	13365	15450	16770
FIU J3	3 days	10910	11132	10794	11848	13212
		7435	11488	11339	10520	11586
		9568	12032	11999	10545	12259
	7 days	14712	13585	14216	13178	15613
		12371	13059	14366	12560	15657
		13556	14015	13620	13694	14495

	28 days	14873	12525	14964	17189	18743
		15850	12493	17031	17473	17909
		14538	16017	16486	16473	19059
	56 days	11849	16485	16080	17932	21315
		15242	12201	14443	16195	18469
		15459	16992	17836	15692	18586

Table 18: OU J3 splitting tensile strength (psi) for each individual specimen for each steel fiber content

Mix	**Age**	**0%**	**1%**	**2%**	**4%**	**6%**
OU J3	**28 days**	1127	1810	2457	3336	2823
		959	1985	2873	2974	2964
		997	2183	2404	2947	2990

Table 19: OU J3 and FIU J3 flexural strength (MOR) (psi) for each individual specimen for each steel fiber content

Mix	Age	0%	1%	2%	4%	6%
OU J3	28 days	1264	1782	2468	3750	4113
		1244	1713	2388	5168	4680
		1290	1806	2501	3924	2574
						2864
	56 days	1701	2304	3104	__	4058
		1846	2768	3047	4600	3756
		1662	2334	2961	3526	4608
					4299	
FIU J3	28 days	1940	2112	2427	4146	4337
		1925	2065	2657	4003	4346
		1659	1633	2378	2616	3801
	56 days	2009	2305	3267	4779	__
		1794	2156	2720	2953	4390
		2085	2087	2412	4461	4586